INTERNATIONAL JOURNAL FOR NUMERICAL METHODS IN FLUIDS, VOL. 8, 247–281 (1988)

LAMINAR NATURAL CONVECTION IN A PARTIALLY DIVIDED RECTANGULAR CAVITY AT HIGH RAYLEIGH NUMBER

KEITH H. WINTERS

Theoretical Physics Division, Harwell Laboratory, Didcot, Oxfordshire, OX11 ORA, U.K.

SUMMARY

Finite element predictions of two-dimensional laminar natural convection in a partially divided rectangular cavity at high Rayleigh number are presented. The walls are differentially heated, the horizontal surfaces are insulated and the cavity contains a partial vertical divider which is centrally located and whose height is varied. Detailed results are presented for an aluminium half-divider in water for Rayleigh number up to 10^{11} and compared directly with recent experiments in a cavity of aspect ratio 1/2. The predicted flow and heat transfer are in good agreement with the measurements and confirm the existence of a high Rayleigh number regime with characteristic behaviour that differs significantly from that found at lower Rayleigh number. In addition, the effects of the divider height, the divider conductivity, the fluid Prandtl number and the cavity aspect ratio are studied. The results show that a direct simulation of the complex flow and heat transfer that occurs in partially divided cavities is possible for realistic physical conditions.

KEY WORDS Natural convection Finite element method High Rayleigh number

INTRODUCTION

This paper presents the results of a simulation of two-dimensional laminar natural convection inside a partially divided rectangular cavity with differentially heated sidewalls at high Rayleigh number. The problem has important applications in the fields of thermal insulation, reactor thermal hydraulics and fire prediction, where Rayleigh numbers greater than 10^{10} are typical and where complex flows can result from the presence of baffles and obstructions.

The study of the effect of a partial divider on the convection in a cavity with sidewall heating has been the subject of several recent and detailed experimental investigations. Duxbury[1] considered the effect of brass partitions in air at Rayleigh numbers Ra up to 10^6 and cavity aspect ratios A from 5/8 to 5. Nansteel and Greif[2,3] and Nansteel[4] studied aluminium and foam partitions in water and silicone oil for $A = 1/2$ and Ra up to 10^{11}. Lin and Bejan[5] investigated double-glazed glass/air panels in water for $A = 0{\cdot}305$ and Ra up to 10^{11}. Bajorek and Lloyd[6] considered Perspex partial dividers in air at $A = 1$ and Ra up to 10^8.

In contrast to the extensive experimental studies, there has been little computational work on this problem, even at low Rayleigh number, unlike the much-studied undivided cavity. This can be attributed to both the complex nature of the geometry and the difficulty of attaining results at the high Rayleigh numbers of the experiments. Chang *et al.*[7] simulated the convection in a square cavity with both floor and ceiling baffles for Rayleigh numbers up to 10^8. In a previous paper, Winters[8] presented results for brass partitions in air, and these were compared directly

0271–2091/88/030247–35$17.50

Received 9 December 1986

with the measurements of Duxbury at $Ra = 10^6$. The predicted and observed flows were in good qualitative agreement, although the predicted Nusselt numbers were higher than the measured values, and the observed flow separation at the divider tip was not found. This work was extended[9] to the case of an aluminium half-divider in a water-filled cavity of aspect ratio 1/2, as studied by Nansteel and Greif. The experiments were performed at high Rayleigh numbers of up to 10^{11}, and the flow patterns and heat transfer differ significantly from the results of Duxbury for air at lower Rayleigh number. Unfortunately, predictions could only be obtained for Rayleigh numbers up to 5×10^9, and a direct comparison with experiments was not possible, although the extrapolated Nusselt numbers agreed well with the measured values.

In this paper we will present results for Rayleigh numbers up to 10^{11} for direct comparison with the experiments of Nansteel and Greif.[2,10] The accurate prediction of laminar natural convection at such high Rayleigh numbers presents a considerable challenge, and no results have been reported hitherto for the partially divided case. The direct simulation of the experiments is possible due to the work of Cliffe *et al.*,[11] who identified and overcame a restriction upon finite element models which had prevented the computation of convection at high Rayleigh number.

It is important to stress that for sidewall heating there is increasing stratification in the regions of low fluid velocity; this has a stabilizing effect and inhibits the transition to turbulence. Thus Nansteel and Greif[2] observed mainly laminar convection in their experiments, and a simulation of laminar conditions is meaningful even at Rayleigh numbers up to 10^{11}. The stabilizing effect of the temperature stratification has also been noted by Bohn *et al.*[12] and Bauman *et al.*[13] The stabilization is enhanced further by heating the roof and/or cooling the floor, and predominantly laminar convection was observed for Rayleigh numbers as high as 5×10^{12} by Kenworthy *et al.*[14] in an experimental study of convection in a component of a Fast Breeder Reactor.

The experimental work on partially divided cavities has raised important questions concerning the effects of the various parameters which determine the convective flow and heat transfer. In particular, there is a discrepancy between the measurements of Nansteel and Greif[2] and Lin and Bejan[5] for an insulating partial divider in water. The experiments were carried out at different aspect ratios, and the role of the aspect ratio on the heat transfer is unclear. Also, Nansteel and Greif[10] found a different heat transfer for an insulating partial divider in silicone oil compared with the same divider in water. Yet previous work on undivided cavities has shown that the heat transferred by oil differs negligibly from that transferred by water, at the same Rayleigh number. We address these questions by considering each of the effects of Rayleigh number, divider height, divider conductivity, fluid Prandtl number and cavity aspect ratio on the laminar natural convection.

THEORY

Basic equations

We consider a rectangular cavity of aspect ratio A, the ratio of height to width, with differentially heated sidewalls and insulated horizontal surfaces. A baffle projects from the mid-point of the floor and partially divides the cavity, as shown in Figure 1. The corresponding case of a vertical partition of the same length projecting from the mid-point of the roof has a related solution in the Boussinesq approximation.[4,8] Graphically, this is obtained by rotating the streamlines and isotherms by 180° about the cavity centre and relabelling the contour values of temperature, as illustrated symbolically in Figure 2.

The flow in the cavity is assumed to be steady, laminar and described by the Navier–Stokes

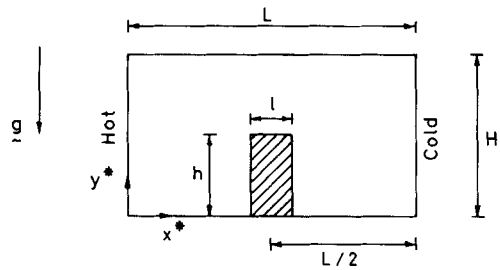

Figure 1. The geometry of the partially divided cavity

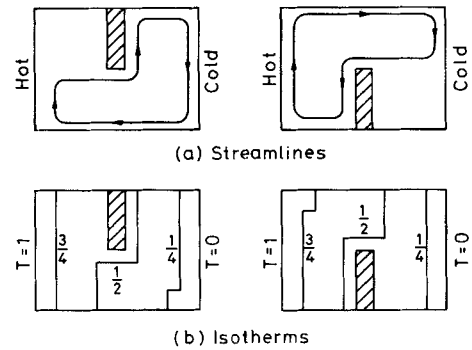

Figure 2. The correspondence between the convection for a vertical partition projecting from the roof and the convection for a partition of the same height projecting from the floor

and energy equations in the Boussinesq approximation. Thus it is important to note that all the results to be presented in this paper are related to those for a partial divider of the same length projecting from the roof. Nansteel[4] verified the validity of the Boussinesq approximation, and therefore the validity of the correspondence shown in Figure 2, for the physical conditions in his experiments and those of Nansteel and Greif.[2]

The governing equations are non-dimensionalized using the following scales:

length scale L, where L is the cavity width;
velocity scale κ/L, where κ is the thermal diffusivity;
temperature scale $(T_H^* - T_C^*)$, where T_H^* and T_C^* are the temperatures of the hot and cold walls;
pressure scale $\rho_0\kappa^2/L^2$, where ρ_0 is the density at the reference temperature T_C^*.

The non-dimensional horizontal and vertical components of velocity, u and v, the pressure p and the temperature T are then given by the following equations:

$$u\frac{\partial u}{\partial x} + v\frac{\partial u}{\partial y} + \frac{\partial p}{\partial x} - Pr\nabla^2 u = 0, \tag{1}$$

$$u\frac{\partial v}{\partial x} + v\frac{\partial v}{\partial y} + \frac{\partial p}{\partial y} - Pr\nabla^2 v = RaPr\,T, \tag{2}$$

$$\frac{\partial u}{\partial x} + \frac{\partial v}{\partial y} = 0, \tag{3}$$

$$u\frac{\partial T}{\partial x}+v\frac{\partial T}{\partial y}-\nabla^2 T=0, \tag{4}$$

where x and y are the non-dimensional co-ordinates x^*/L and y^*/L.

These equations contain two non-dimensional parameters, the Rayleigh number (based on cavity width)

$$Ra=g\beta(T_H^*-T_C^*)L^3/\kappa\nu$$

and the Prandtl number

$$Pr=\nu/\kappa,$$

where ν is the kinematic viscosity, β the coefficient of volumetric expansion and g the acceleration due to gravity.

Other parameters which enter into this study are:

aspect ratio $A=H/L$, where H is the cavity height;
relative divider height $d=h/H$, where h is the divider height;
aperture $A_p=1-d$.

In all cases the non-dimensional divider thickness $t=l/L$ was 0·031, as in the experiments of Nansteel and Greif.

The finite conductivity of the partition is taken into account in this work, so that the contrasting cases of an insulating and conducting partial divider can be studied. Inside the solid partition the temperature is given by

$$k_r\nabla^2 T=0, \tag{5}$$

where k_r is the conductivity of the partition relative to the fluid. This equation for the solid region is solved simultaneously with the flow and energy equations (1)–(4) for the fluid region. The relative conductivity k_r is retained in equation (5) to ensure continuity of heat flux across the solid/fluid interface.

As an aid to flow visualization, the streamfunction is calculated from

$$\nabla^2 s=\frac{\partial u}{\partial y}-\frac{\partial v}{\partial x} \tag{6}$$

using the finite element interpolation of the computed u and v components of velocity.

The boundary conditions are the usual Dirichlet no-slip and pressure reference point conditions for the velocity and pressure:

$u=v=s=0$ over the entire boundary;

$p=0$ at an interior point.

The temperature boundary conditions are:

$T=1$ on the left vertical wall;
$T=0$ on the right vertical wall;
$\partial T/\partial y=0$ on the horizontal surfaces.

In addition, the components of velocity u and v and the streamfunction s are set equal to zero on the surface of the divider.

The heat transfer across the cavity is given by the average value of the Nusselt number

$$\overline{Nu} = \frac{1}{A}\int_0^A Nu\,\mathrm{d}y, \tag{7}$$

where the local Nusselt number

$$Nu = \partial T/\partial x$$

is evaluated at either $x = 0$ or $x = 1$. It is important to note that the definitions of Rayleigh number and Nusselt number used throughout this paper are based on cavity *width*.

Finally it should be pointed out that the partition has a conducting or insulating effect depending on the value of its non-dimensional conductance k_d, rather than its relative conductivity k_r.[2] The conductance is defined as

$$k_d = k_r(L/l)/\overline{Nu}, \tag{8}$$

where l is the partition thickness. The divider is non-conducting if $k_d \ll 1$ or conducting when $k_d \gg 1$. These two criteria are satisfied respectively for the aluminium and foam dividers in the experiments of Nansteel and Greif,[2] for which $k_r = 350$ for aluminium in water and $k_r = 0{\cdot}05$ for foam in water.

Finite element formulation

The equations and boundary conditions were solved in a standard Galerkin formulation of the finite element method. Previous applications of the finite element method to natural convection have been limited in terms of the maximum Rayleigh number that could be achieved, and 10^7–10^8 has often been regarded as a high Rayleigh number representing a difficult computational problem. Winters[9] was able to obtain predictions at 5×10^9 in a previous study, with a very fine mesh, but was unable to achieve converged results at higher Rayleigh number.

Cliffe *et al.*[11] identified a limitation on the maximum Rayleigh number that could be attained in their finite element formulation. The problem occurs due to the characteristic nature of the convection at high Rayleigh number; the flow is concentrated in narrow boundary layers, outside which the fluid stagnates with a high degree of temperature stratification. The equations describing the flow and heat transfer in the stagnant region then reduce to a simple balance between the vertical pressure gradient and the buoyancy force. Most commonly used elements have too few degrees of freedom to achieve this balance accurately, resulting in spurious mesh scale oscillations in the vertical velocity. The magnitude of these oscillations increases with Rayleigh number and ultimately prevents convergence unless an unrealistically fine mesh is used in the *stagnant* region.

Cliffe *et al.* demonstrated how the problem might be overcome by implementing a certain element, a nine-noded quadrilateral with a piecewise-linear variation of the pressure. The extra pressure freedoms ensure an exact balance between pressure gradient and buoyancy terms, provided that the elements are rectangular and parallel to the isotherms. With this new element there was no difficulty in simulating convection in rectangular enclosures at Rayleigh numbers up to 10^{12}, using relatively coarse grids. The element was used successfully by Kenworthy *et al.*[14] in a joint experimental and computational study of convection in a rectangular plenum at a Rayleigh number of 5×10^{12}.

All computations in the present study were carried out on a CRAY-1S computer, using the ENTWIFE package, which is based on the TGSL library of finite element subroutines developed at Harwell. The finest grid used consisted of 86 by 40 elements in the x and y directions respectively, with a suitable grading of the element spacing to resolve the extremely narrow boundary layers

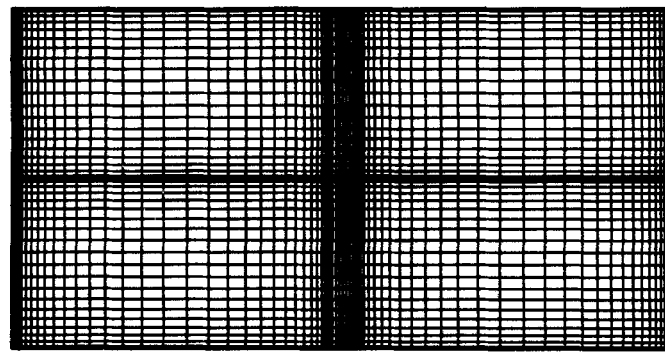

Figure 3. Finite element grid of 86 × 40 nine-noded quadrilateral elements

which arise at high Rayleigh number. This is denoted an 86 × 40 grid and is shown in Figure 3 for the case of a partial or complete divider. As an example of the grading, it has the effect of placing the $(n+1)$th vertical element boundary at a distance of $0{\cdot}25 \times (0{\cdot}0485n)^3$ from the left sidewall, for $n < 20$. A different grid was used for an undivided cavity, with the elements graded only towards the outer boundaries. The non-linearities in the equations were treated by a Newton–Raphson procedure, and the linear equations at each iteration were solved by the frontal method. The initial guess for the Newton–Raphson iterations was the converged solution at a lower Rayleigh number. The CPU time required for each Newton–Raphson iteration was around 110 s on the grid of Figure 3, of which 92 s was spent in the frontal solver. No more than six iterations were needed at each Rayleigh number.

RESULTS

The effect of Rayleigh number

We consider firstly an aluminium partial divider of height $h = 1/2$ in a water-filled cavity of aspect ratio $A = 1/2$, as studied by Nansteel and Greif.[2] A Prandtl number of 3·5 is assumed for water, and the conductivity of aluminium relative to water is taken as $k_r = 350$. We simulated the convection by increasing the Rayleigh number progressively, as described in the previous section. The values of Rayleigh number chosen are given in Table I, which also records the finest grid used at each Ra. Small steps in Ra were essential in the range $10^{10} \leqslant Ra \leqslant 10^{11}$ in order for the Newton–Raphson procedure to converge.

Figure 4 shows a series of contour plots of the predicted streamfunction and temperature, for Rayleigh numbers from 10^6 to 10^{11}. Results at smaller Rayleigh number are not shown; for sufficiently small Ra the streamlines are disposed symmetrically about the vertical mid-line, and the isotherms are almost vertical and equally spaced (the deviation being due to the different thermal conductivities of the fluid and divider). At $Ra = 10^6$ the convection is sufficiently strong to produce a markedly asymmetric flow pattern of two eddies, with the recirculation on the hot side being the stronger. The isotherms are stratified away from the boundaries, reflecting the low velocity in the core of the flow. The effect of the divider is to raise the temperature in the upper half of the cavity; the roof is mostly at a non-dimensional temperature of around 0·6. The streamlines and isotherms are similar to those observed by Duxbury[1] and predicted by Winters[8] for a brass half-divider in air, for $A = 5/8$ and Ra around 10^6.

As the Rayleigh number increases, the eddy on the hot side strengthens, and the flow penetrates

Table I. Heat transfer in a water-filled cavity of aspect ratio 1/2 with an aluminium partial divider of aperture 1/2 for different Rayleigh numbers

Rayleigh number	Grid	Predicted $\overline{Nu}$	Measured* $\overline{Nu}$
10^5	34 × 16	2·36	—
10^6	34 × 16	7·06	—
10^7	34 × 16	15·8	—
5×10^7	34 × 16	25·1	—
10^8	34 × 16	30·5	—
5×10^8	30 × 14	47·5	—
10^9	70 × 32	56·2	—
3×10^9	70 × 32	74·9	—
5×10^9	38 × 18	85·6	—
6×10^9	70 × 32	89·5	—
10^{10}	86 × 40	102	114
2×10^{10}	86 × 40	122	133
3×10^{10}	86 × 40	135	146
5×10^{10}	86 × 40	153	164
7×10^{10}	86 × 40	167	177
8×10^{10}	86 × 40	173	182
9×10^{10}	86 × 40	178	187
10^{11}	86 × 40	183	192

* Reference 2.

less into the cold lower right of the cavity, which is shielded from the hot wall by the partial divider. From $Ra = 10^7$ to 10^9 there is increasing separation of the flow down the cold wall, as the fluid decelerates on approaching the stratified lower right region. This is accompanied by the development of a recirculation in the lower right region and suppression of the original eddy, adjacent to the cold wall, which was seen at $Ra = 10^6$.

At $Ra = 10^9$ there is parallel flow from the hot to the cold walls over much of the upper half of the cavity, with a cold jet returning from the cold wall to the divider tip at mid-height. The isotherms are strongly stratified away from the boundaries, and there is a sharp increase in the vertical temperature gradient to the right of the divider tip. The flow and thermal boundary layers on the vertical surfaces are well established; this is well illustrated in the isometric plots of Figure 5, which give the distribution of the temperature and vertical component of velocity throughout the cavity. The nodes of the finite element grid are located at the intersections of the lines of constant x and y. The isometric view of the v velocity shows the extremely narrow boundary layers, separated by large regions of small vertical velocity, and the regions of flow reversal outside these layers. The isometric view of the temperature shows the sharp gradients at the surfaces and the distinct regions of stable stratification in the interior.

The Rayleigh number of 10^9 marks the start of a distinct regime of flow and heat transfer which is quite different to that found at lower Rayleigh numbers. As the Rayleigh number increases still further to 10^{11}, the features described above are accentuated, with increasingly parallel flow, stratification and intensification of the cold jet. These characteristics are in excellent agreement with the flow visualizations of Nansteel and Greif[2] and Lin and Bejan.[5]

Figure 6 shows the development of the predicted temperature profile along two vertical lines at $x = 1/4$ and 3/4, that is, halfway between the divider and the hot and cold walls respectively, as Ra increases from 10^6 to 10^{11}. The trend towards a universal temperature profile at large Ra is apparent, in agreement with the observations of Nansteel and Greif.[2] The sharp temperature

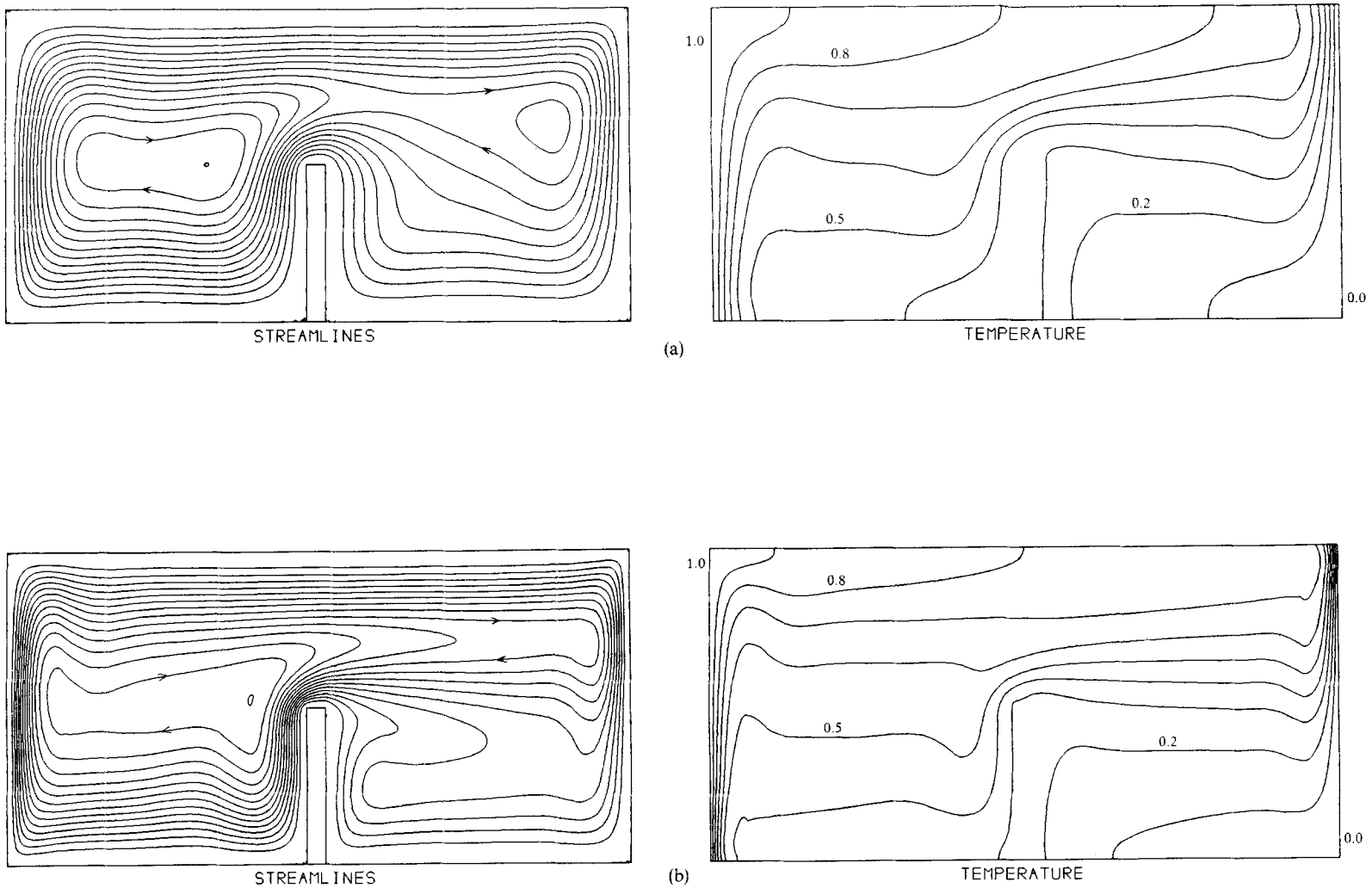

Figure 4. The predicted streamlines and isotherms at Rayleigh numbers of (a) 10^6, (b) 10^7, (c) 10^8, (d) 10^9, (e) 10^{10} and (f) 10^{11}, for a water-filled cavity of aspect ratio 1/2 with an aluminium 1/2-divider

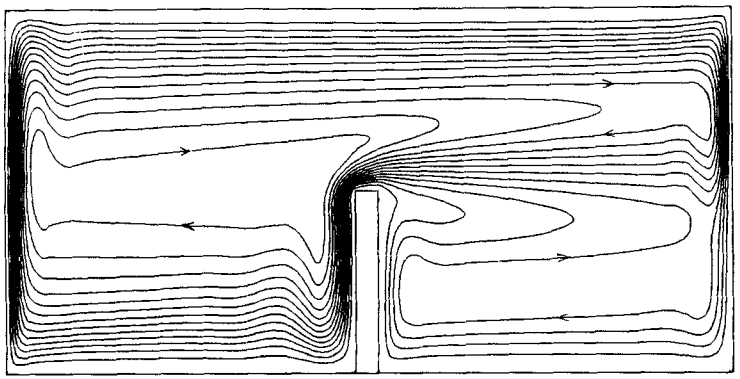

STREAMLINES

(c)

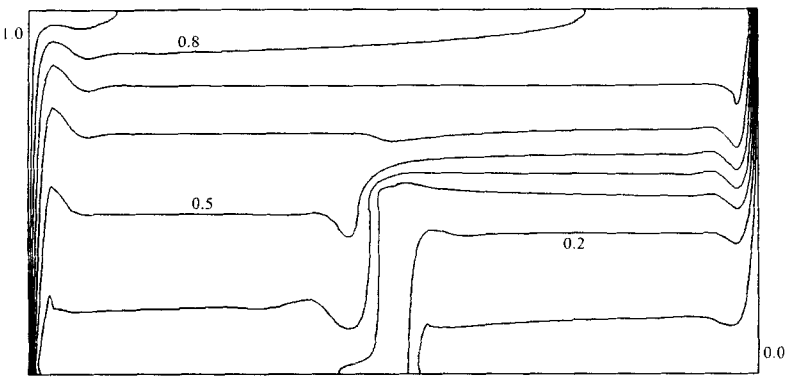

TEMPERATURE

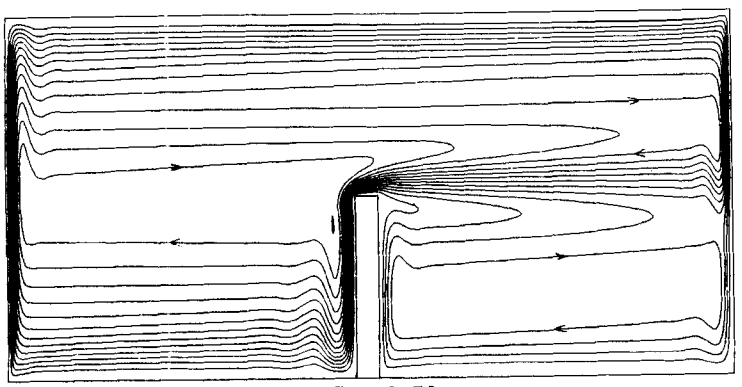

STREAMLINES

(d)

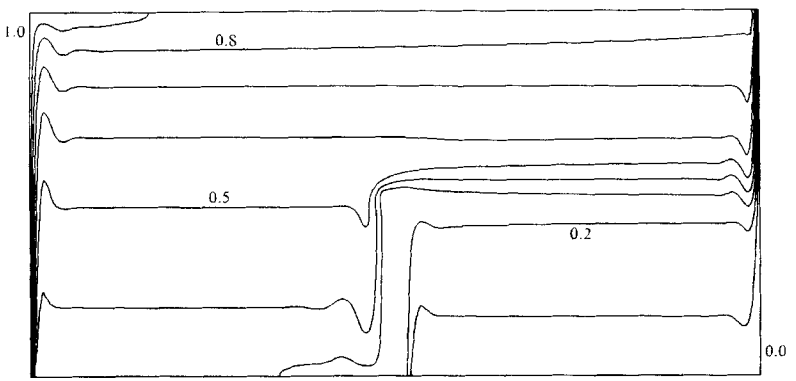

TEMPERATURE

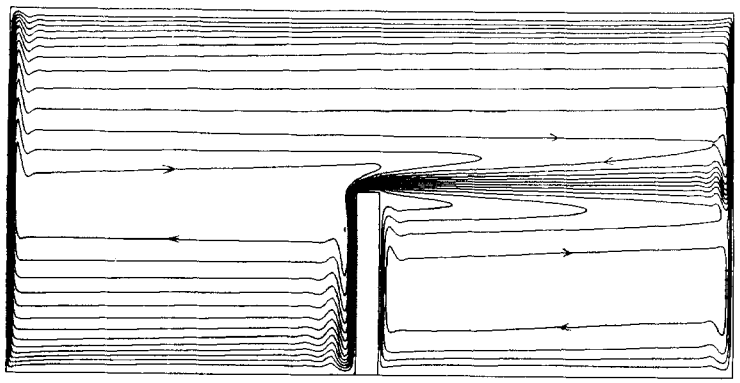

STREAMLINES

(e)

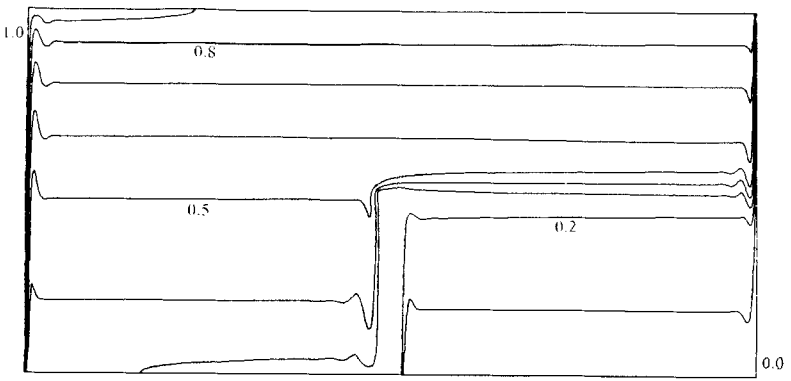

TEMPERATURE

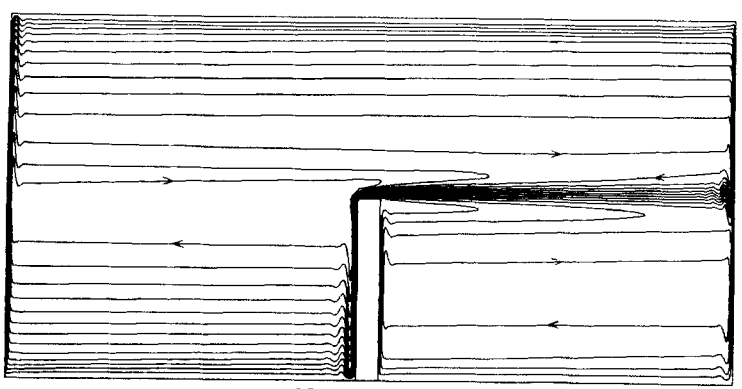

STREAMLINES

(f)

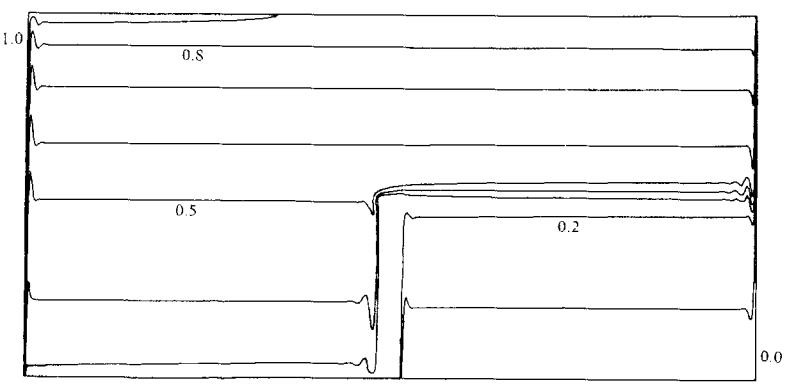

TEMPERATURE

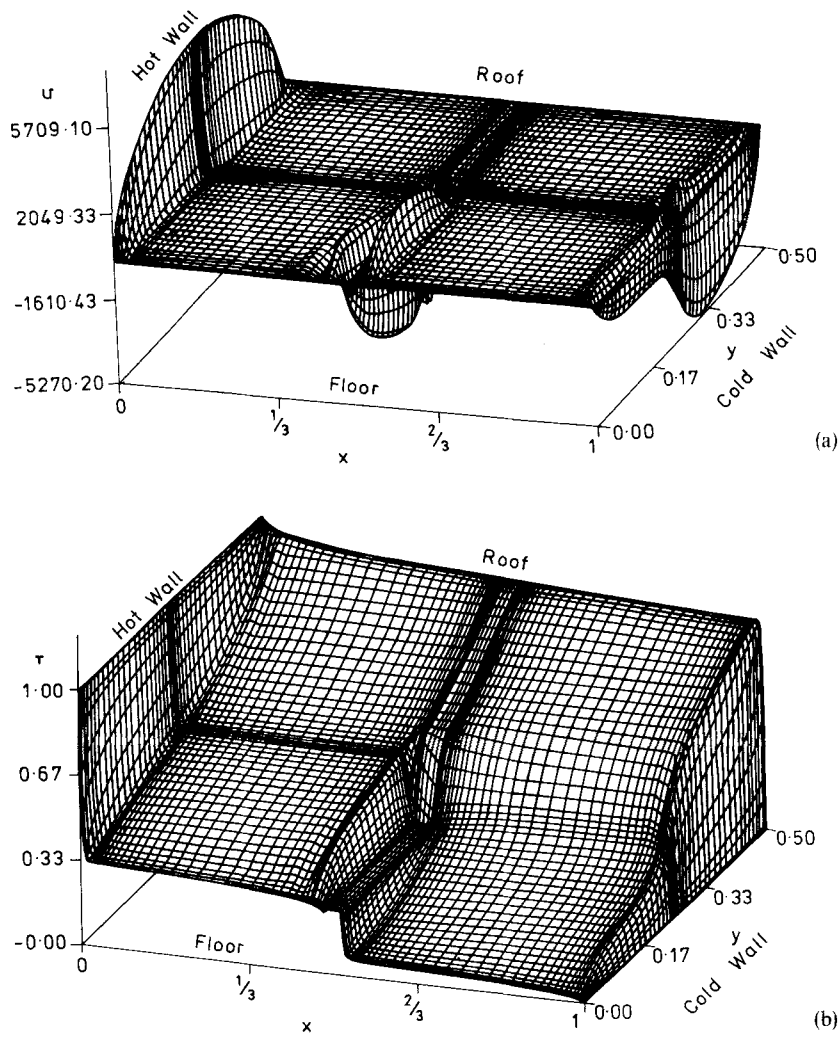

Figure 5. Isometric view of (a) the vertical component of velocity v and (b) the temperature T as a function of x and y for a water-filled cavity of aspect ratio 1/2 with an aluminium 1/2-divider at a Rayleigh number of 10^9

gradient to the right of the divider tip shows clearly in the profile at $x = 3/4$. In the limit of low Rayleigh number, it should be noted that the profiles tend to approximately constant values.

As regards the heat transfer at the walls, Figure 7 shows the variation of the local Nusselt number along the hot and cold walls for Rayleigh numbers from 10^6 to 10^{11}. The local Nusselt number near the base of the hot wall and the top of the cold wall attains a large value at $Ra = 10^{11}$, and considerable thermal stress can be anticipated in those regions. We note that the analysis of Betts and Haroutunian[15] shows that the maxima cannot occur exactly in the corners. The partial divider has a considerable effect on the variation of Nu on the cold wall, and suppresses the Nusselt number below the level of the divider tip while enhancing it above, to give a complex distribution. In contrast, the partial divider seems to have little effect on the variation of Nu along the hot wall.

The overall heat transfer is shown in Figure 8, which presents the variation of lg $\overline{Nu}$ with lg Ra. A simple power law relationship between $\overline{Nu}$ and Ra would result in a straight line on the figure.

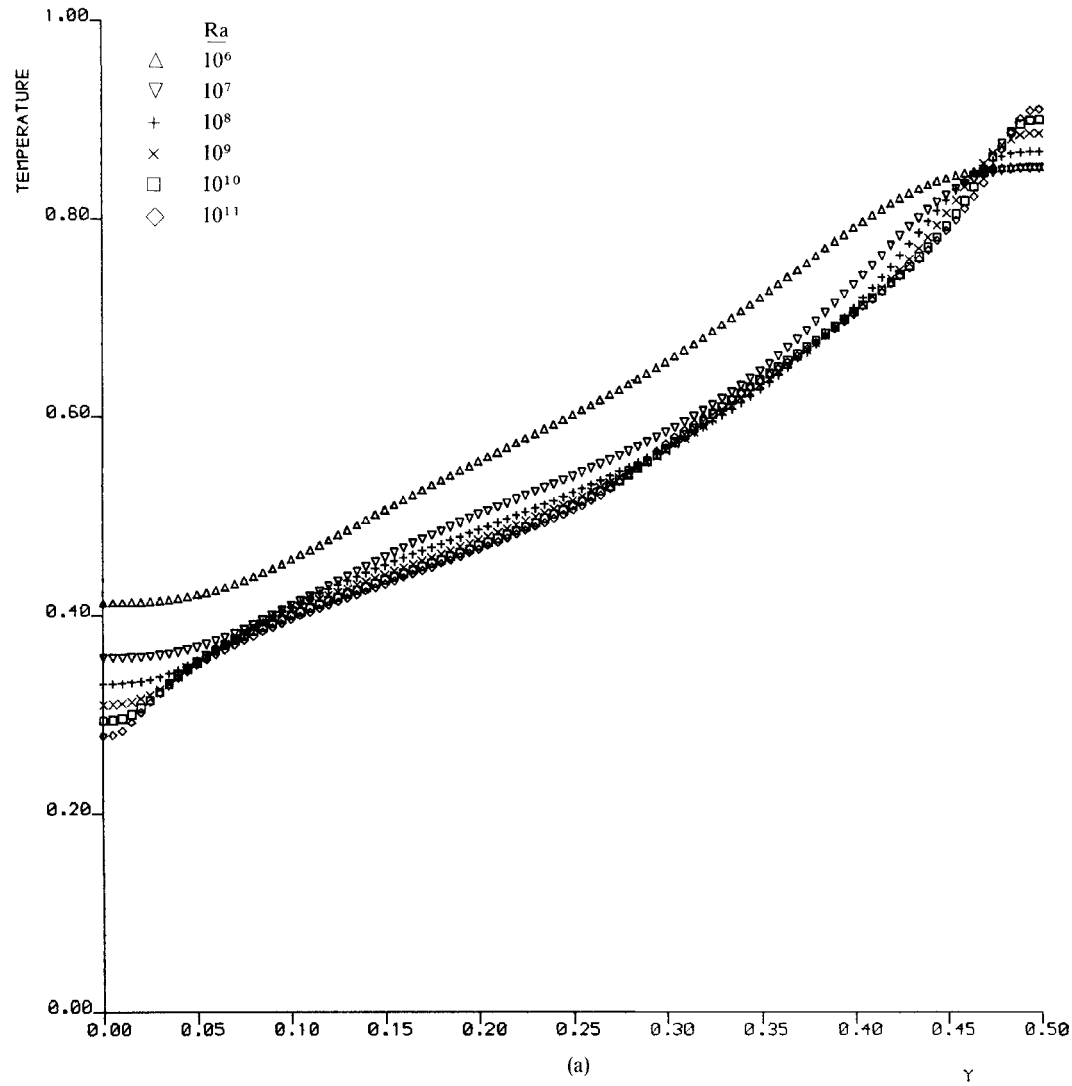

Figure 6. The predicted variation of temperature with height at (a) $x = 1/4$ and (b) $x = 3/4$ for different Rayleigh numbers for a water-filled cavity of aspect ratio 1/2 with an aluminium 1/2-divider. Note that the top of the cavity is at $y = 1/2$

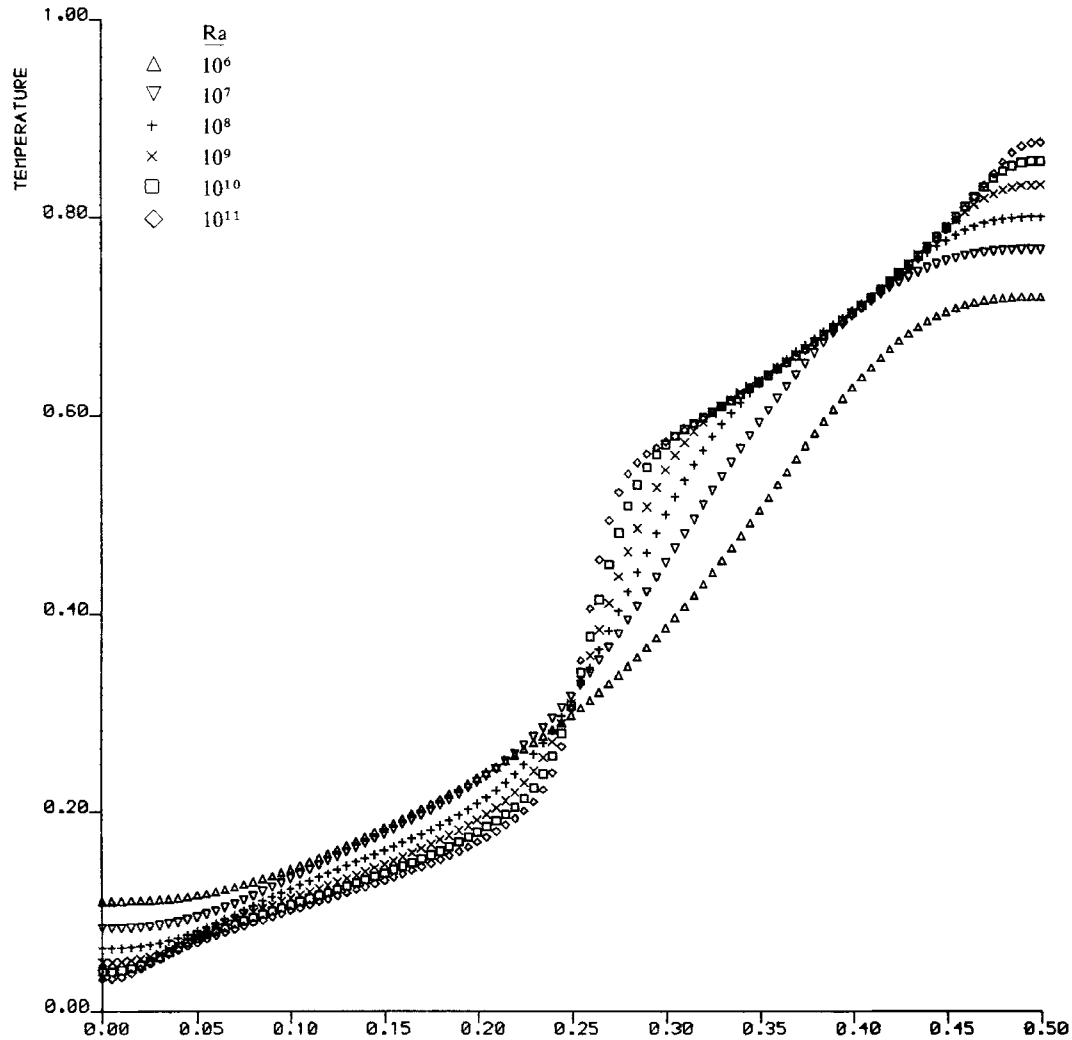
Ra
10⁶
10⁷
10⁸
10⁹
10¹⁰
10¹¹
TEMPERATURE
1.00
0.80
0.60
0.40
0.20
0.00
0.00
0.05
0.10
0.15
0.20
0.25
0.30
0.35
0.40
0.45
0.50
Y

(b)

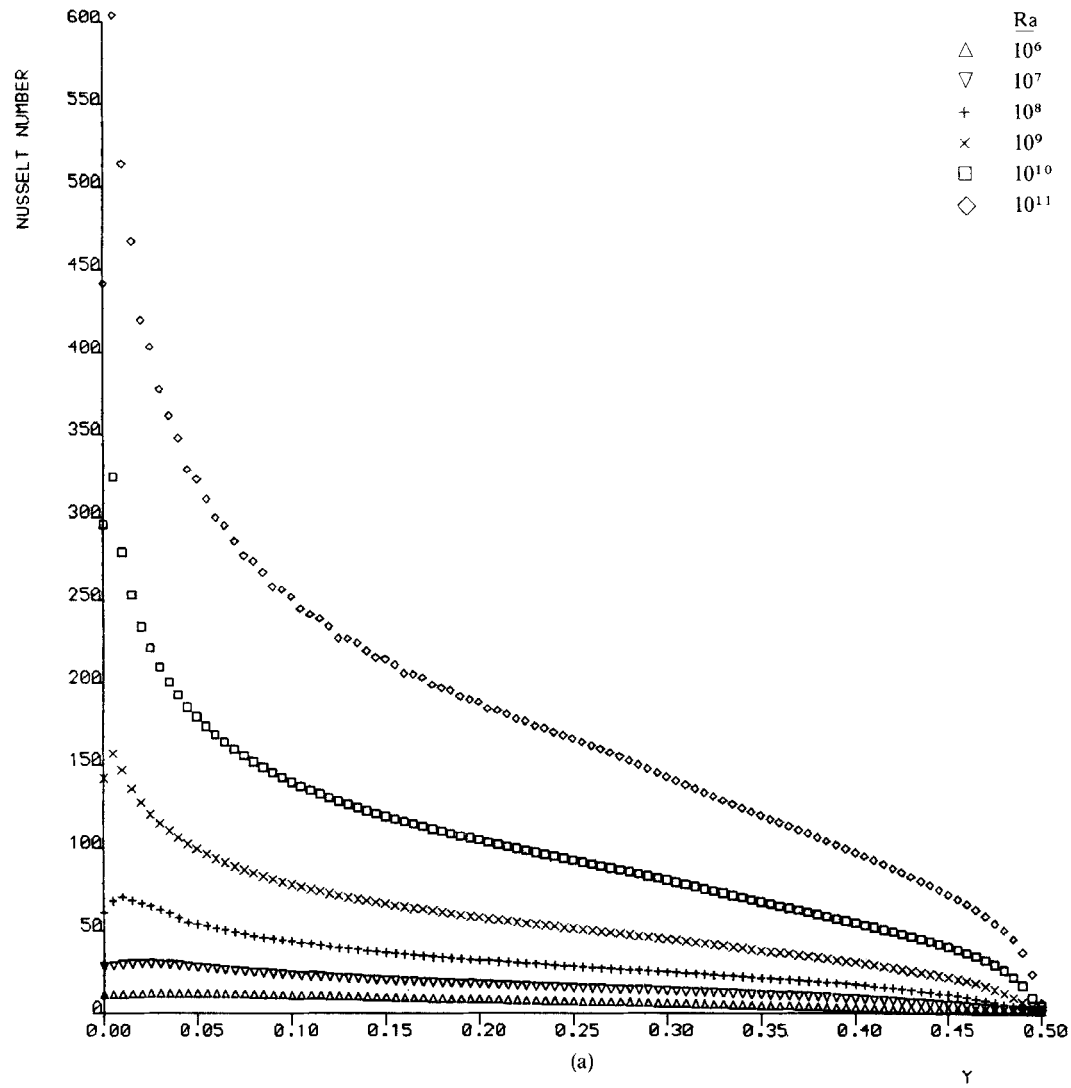

Figure 7. The predicted variation of Nusselt number with height at (a) $x = 0$ (the hot wall) and (b) $x = 1$ (the cold wall) for different Rayleigh numbers for a water-filled cavity of aspect ratio 1/2 with an aluminium 1/2-divider. Note that the top of the cavity is at $y = 1/2$

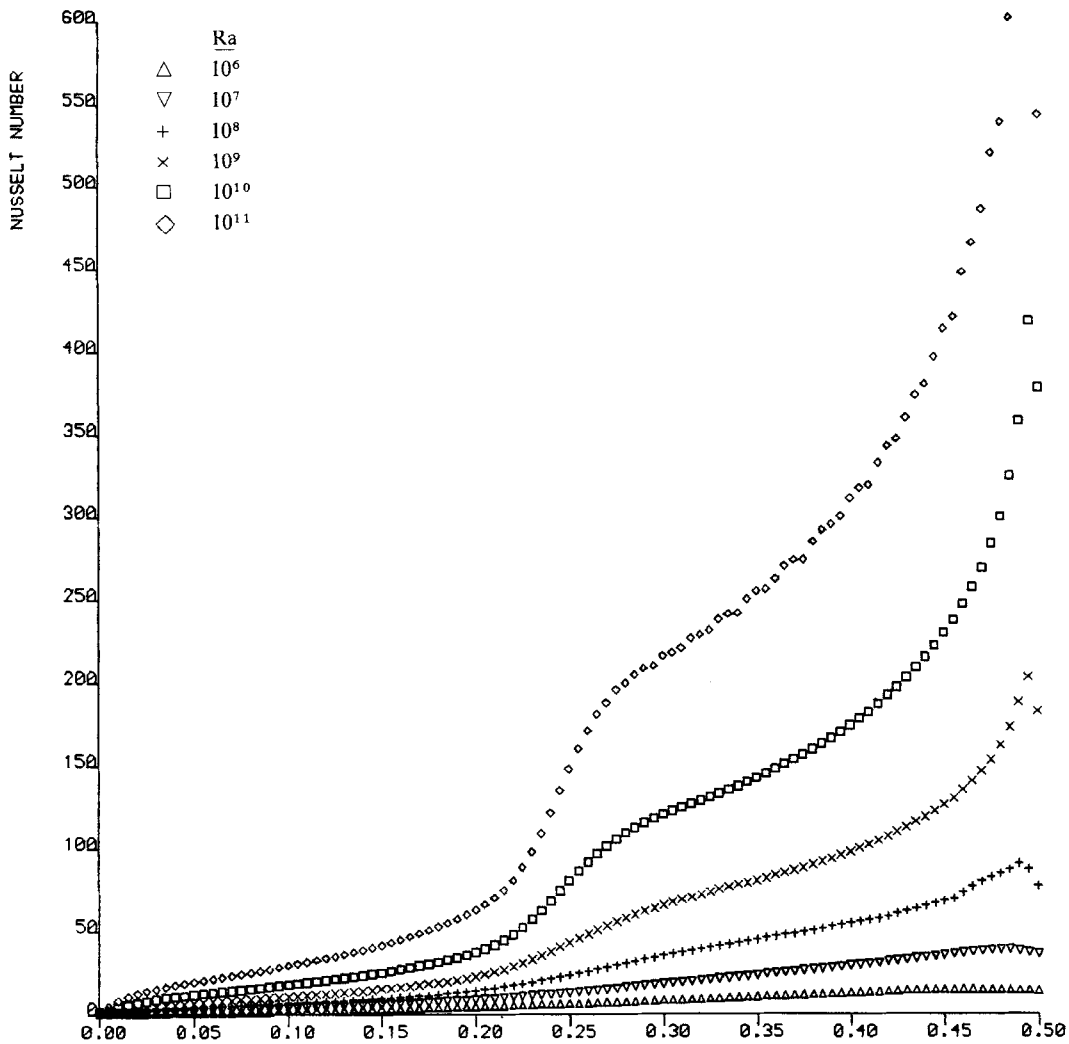
NUSSELT NUMBER
Ra
10^6
10^7
10^8
10^9
10^{10}
10^{11}
600
550
500
450
400
350
300
250
200
150
100
50
0
0.00
0.05
0.10
0.15
0.20
0.25
0.30
0.35
0.40
0.45
0.50
Y

(b)

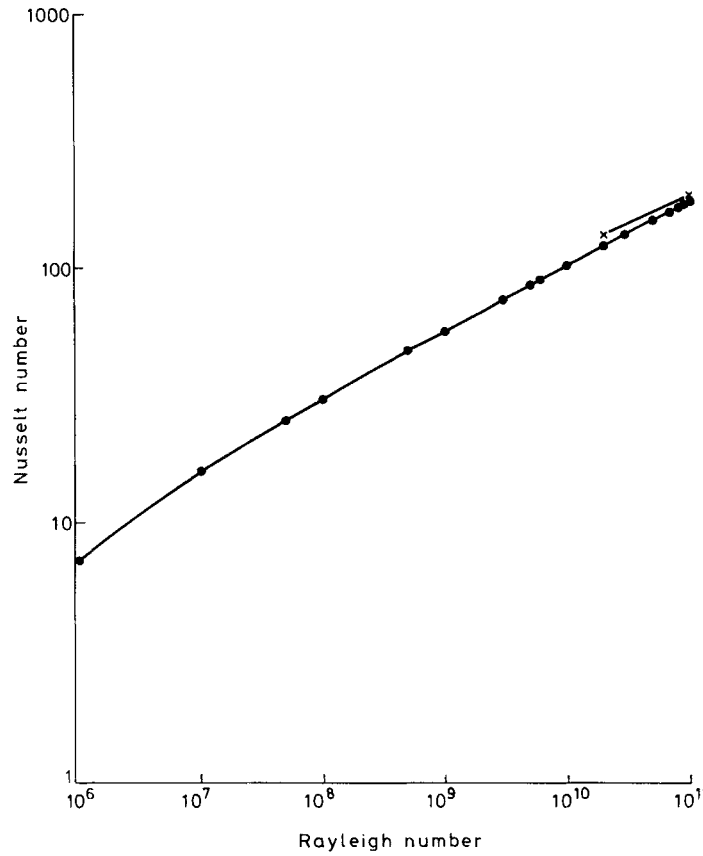

Figure 8. The variation of the average Nusselt number with Rayleigh number for a water-filled cavity of aspect ratio 1/2 with an aluminium 1/2-divider: ●, predicted; ×, correlation of Nansteel and Greif[2]

There is clearly some deviation from linearity at smaller Rayleigh number, and a single power law relation is inappropriate over the range of Rayleigh numbers from 10^6 to 10^{11}. However, in the high Rayleigh number regime, $10^9 \leqslant Ra \leqslant 10^{11}$, there is a considerable degree of linearity, and the relationship is well described by

$$\overline{Nu} = 0{\cdot}286\, Ra^{0.255},$$

which fits the predicted values to better than 0.6%. Figure 8 also includes the results of Nansteel and Greif,[2] displayed as the correlation

$$\overline{Nu} = 0{\cdot}626\, Ra^{0.226}.$$

The agreement with the measurements is very good and within the limits of experimental error. The measured Nusselt number is 12% higher than the predicted value at $Ra = 10^{10}$ and 5% higher at $Ra = 10^{11}$. However, the present predictions show a larger increase in heat transfer with Rayleigh number than the measurements. Gadgil *et al.*[16] also found a larger increase of $\overline{Nu}$ with Ra than Nansteel and Greif[2] for the different case of an undivided cavity.

The present predictions of the average Nusselt number are summarized in Table I. It should be noted that the 86 × 40 grid was necessary to obtain accurate streamlines and isotherms in the bulk of the fluid. However, the prediction of $\overline{Nu}$ was much less sensitive to the size of grid. For example,

an average Nusselt number of 102 was obtained at $Ra = 10^{10}$ for grids of 50 × 24, 70 × 32 and 86 × 40 elements.

The effect of partition height

We now consider the effect of varying the aperture A_p left by the partial divider, between the two extremes of $A_p = 0$ and 1, representing a completely divided and undivided cavity respectively. Figure 9 shows a series of contour plots of predicted streamfunction and temperature for the aluminium divider in a water-filled cavity of aspect ratio 0·5 at $Ra = 10^9$ for apertures of 0, 1/4, 1/2, 3/4 and 1.

In the case of the complete divider, $A_p = 0$, the symmetry of the streamlines through rotation by 180° is clear. The partial divider has a dramatic effect on the flow in the right, colder half of the cavity as the aperture increases from zero. For small apertures, the cold jet which separates from the cold wall at the level of the divider tip is relatively weak, and much of the flow penetrates the lower right section. For $A_p = 1/4$ two strong boundary layers are evident on the lower cold wall and the right face of the divider. The flow in the region shielded from the hot wall by the divider resembles that in an undivided cavity. As the aperture increase, the cold jet intensifies, and there is a corresponding reduction in the flow which penetrates the lower right section of the cavity, and a weakening of the boundary layers there.

On the left, hotter side of the cavity, the divider has much less effect on the flow, the most noticeable effect being the displacement of the core of the recirculation according to the height of the partial divider. There are strong boundary layers on the hot wall and left face of the divider, for all apertures.

The effect of aperture on the isotherms is also more pronounced in the right half of the cavity. For $A_p = 1/4$ there is a large vertical temperature gradient at the level of the divider tip, shown by the closeness of the 0·4 and 0·7 isotherms, and this local gradient decreases as the aperture increases. The roof temperature in the right half shows a large increase on increasing the aperture from 0 to 1/4, and then changes little as the aperture increases further to 1. The temperature of the floor, on the other hand, is small in the right half for all apertures from 0 to 3/4, increasing slightly for the undivided cavity. The thermal boundary layer on the cold wall extends from the roof to the level of the partial divider, and we shall see that this is reflected in the distribution of the local Nusselt number on this wall. The most significant effect of the partial divider on the temperature in the left half of the cavity is to be found at the floor, which becomes progressively colder as the aperture increases.

Temperature profiles along the vertical lines at $x = 1/4$ and 3/4 are given in Figure 10. These show more clearly the dependence of temperature on height above the floor in each half of the cavity for different apertures. Considering the $x = 1/4$ profiles first, the temperature is higher everywhere for the completely divided cavity $A_p = 0$, as expected. For non-zero apertures the temperature variation above the level of the divider tip is identical to that of the undivided cavity, regardless of aperture. Below the divider tip the temperature variation for each aperture is similar, and the floor temperature progressively decreases as the aperture increases. At $x = 3/4$ the temperature variation for the partially divided cavity comprises two distinct regions. Below the divider tip the temperature is close to that of the completely divided cavity $A_p = 0$ for all apertures, while above the divider tip it is close to that of the undivided cavity $A_p = 1$, with a rapid increase in temperature at the level of the divider tip.

Figure 11 shows the distribution of the local Nusselt number along the hot and cold walls for different apertures. The Nusselt number on the hot wall increases with aperture; the largest change occurs at the base, with a much smaller variation in the upper section, except at $A_p = 0$. The

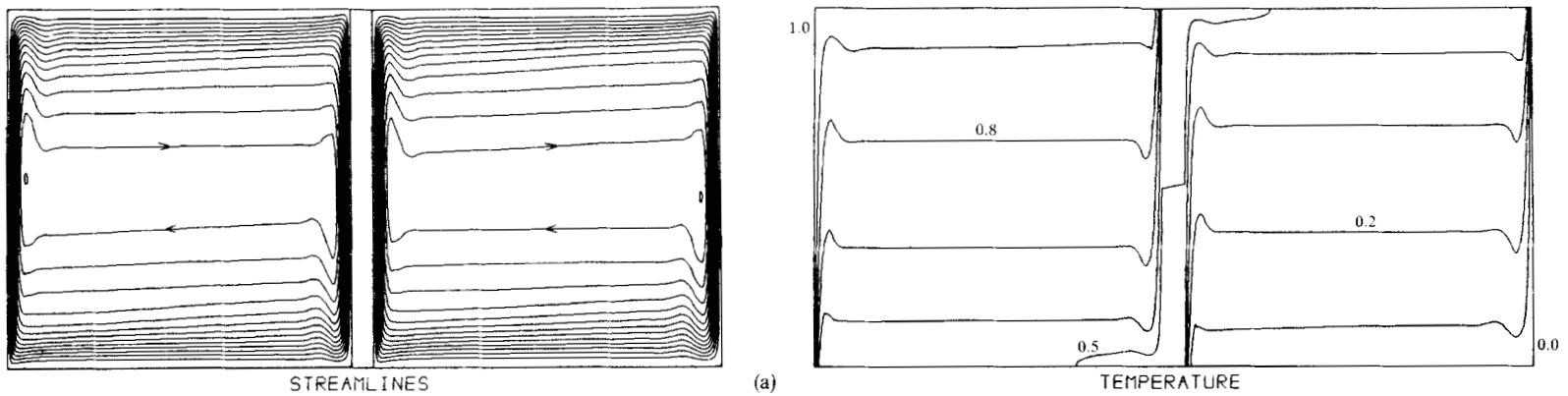

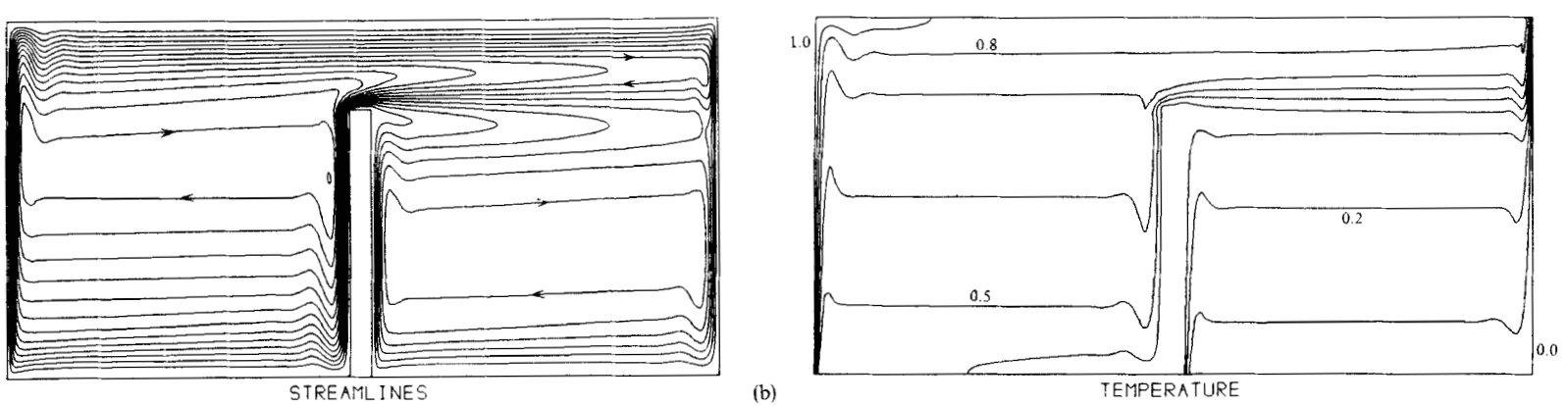

Figure 9. The predicted streamlines and isotherms at apertures of (a) 0, (b) 1/4, (c) 1/2, (d) 3/4 and (e) 1 for a water-filled cavity of aspect ratio 1/2 at a Rayleigh number of 10^9

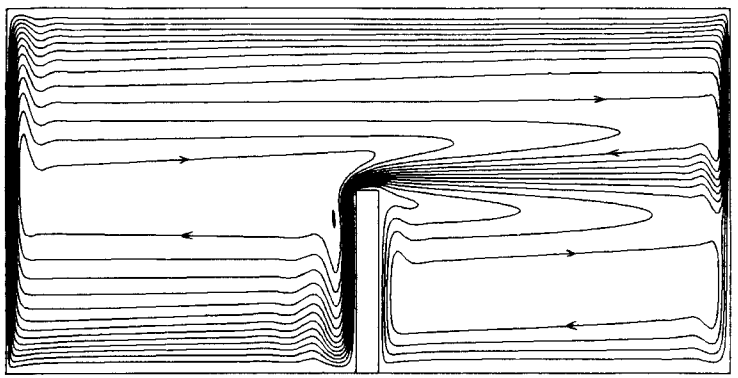

STREAMLINES

(c)

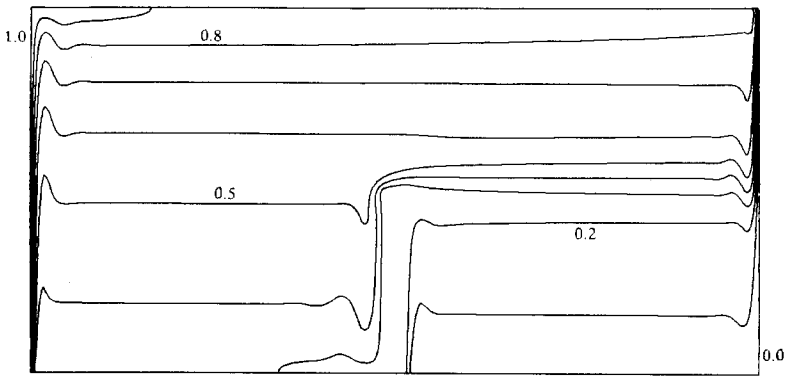

TEMPERATURE

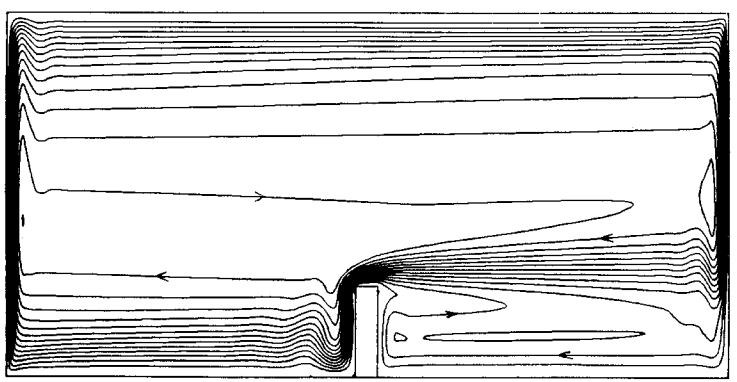

STREAMLINES

(d)

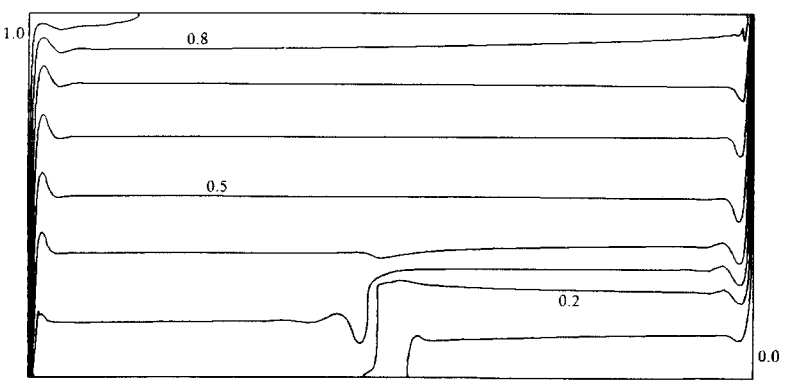

TEMPERATURE

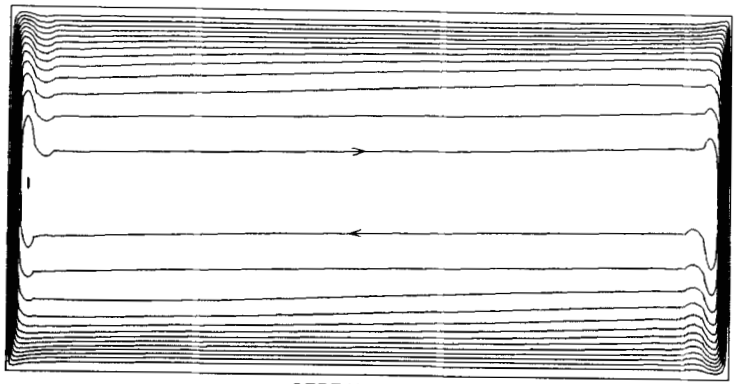

STREAMLINES

(e)

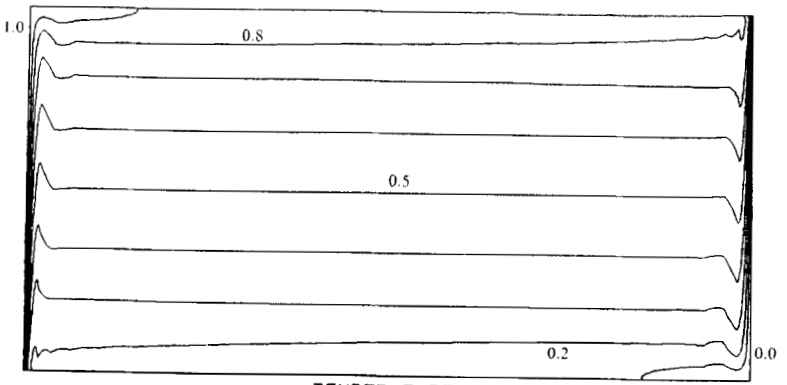

TEMPERATURE

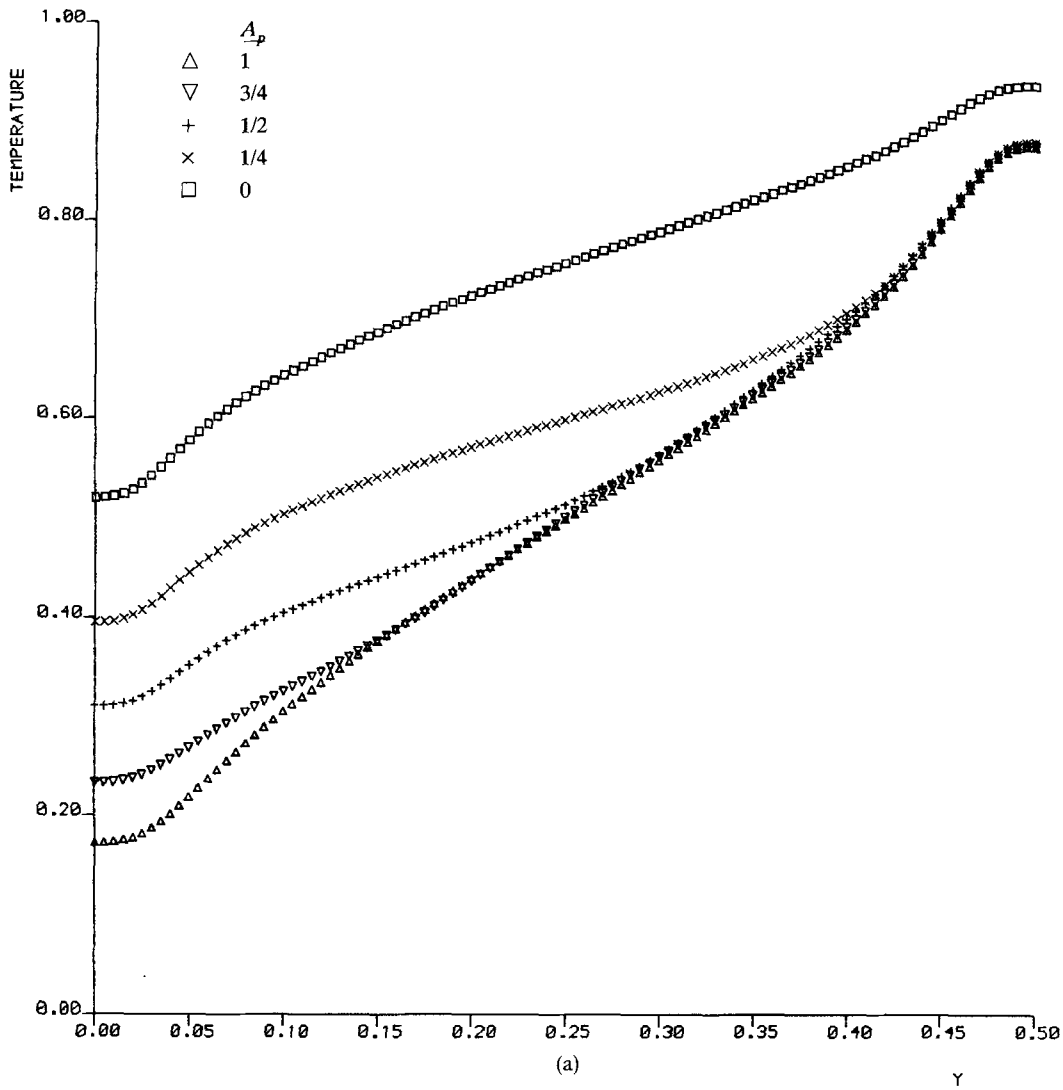

Figure 10. The predicted variation of temperature with height at (a) $x = 1/4$ and (b) $x = 3/4$ for different apertures for a water-filled cavity of aspect ratio 1/2 with an aluminium partial divider at a Rayleigh number of 10^9. Note that the top of the cavity is at $y = 1/2$

distribution along the cold wall is similar to that of the temperature, with the local Nusselt number being close to that of the divided cavity below the level of the divider tip, and close to that for the undivided cavity above it.

Figure 12 shows the dependence of the overall heat transfer on Rayleigh number for each of the apertures. Except for $A_p = 1/4$, the slope of each curve is similar. Figure 13 represents the behaviour of the overall heat transfer in a different way, showing the dependence on aperture for each Rayleigh number. At high Rayleigh number the change in Nusselt number is small as the aperture is decreased from 1 to 1/2, but there is an increasingly greater effect as the aperture decreases further to 0. For example, at $Ra = 10^9$ the 1/2-divider reduces the heat transfer in the

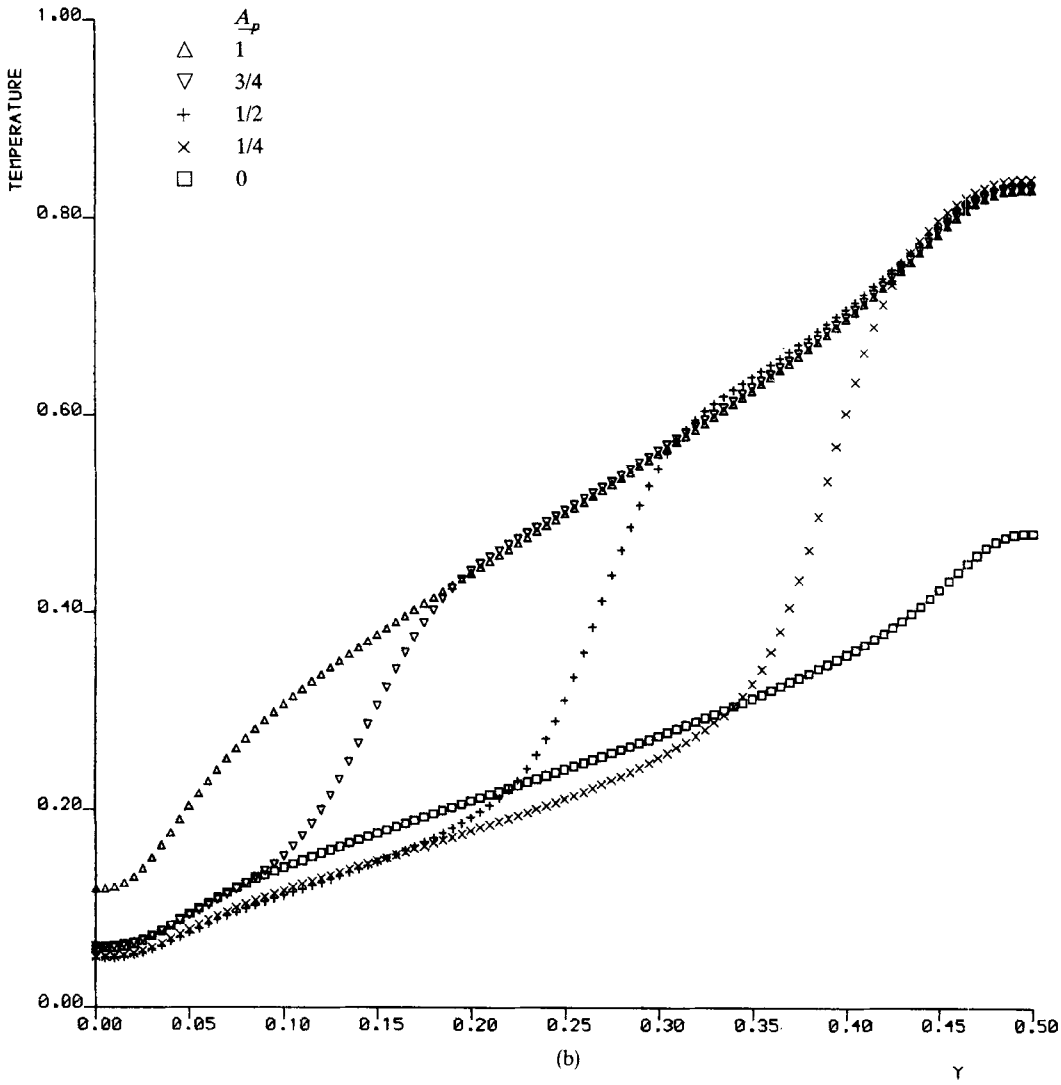
A_p
1
3/4
1/2
1/4
0
TEMPERATURE
1.00
0.80
0.60
0.40
0.20
0.00
0.00
0.05
0.10
0.15
0.20
0.25
0.30
0.35
0.40
0.45
0.50
Y

(b)

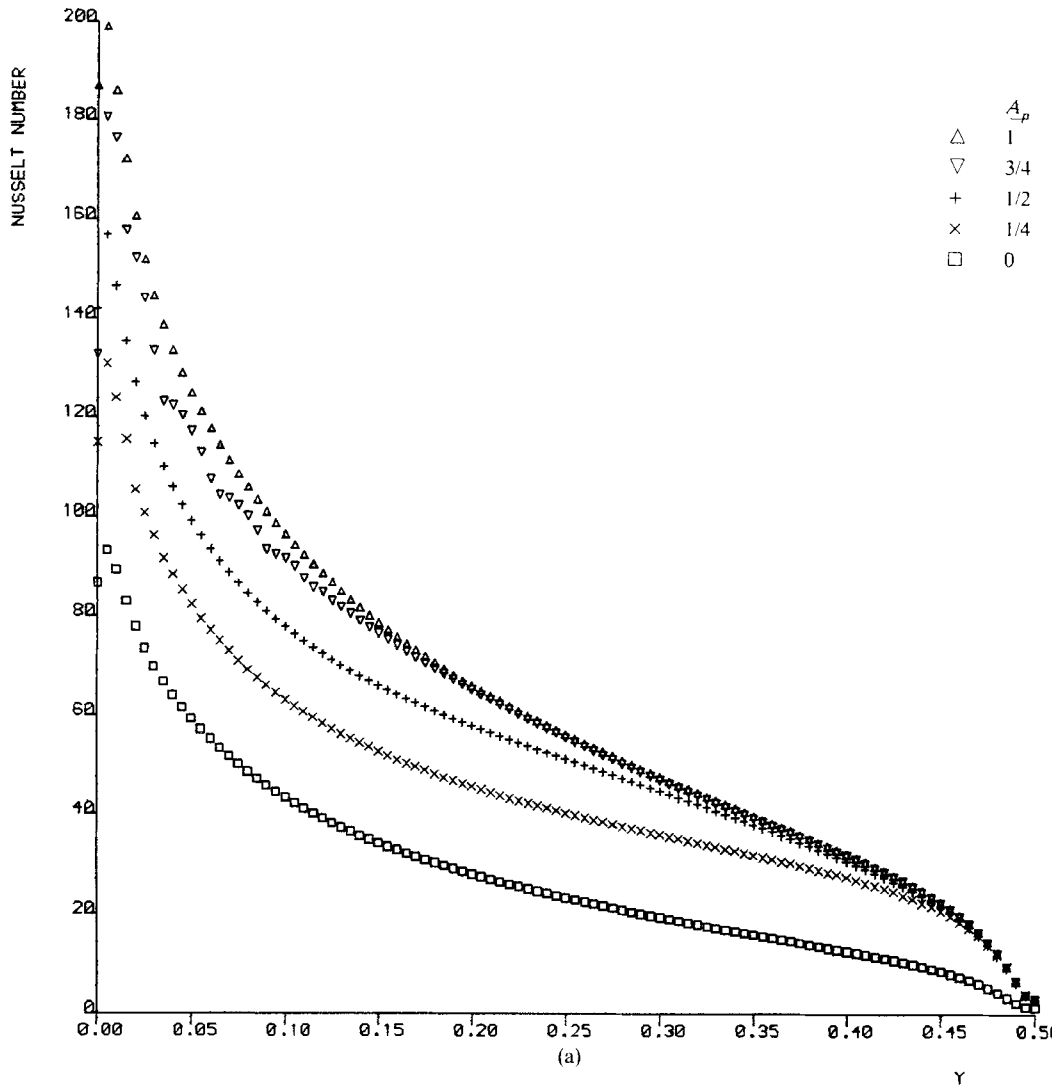

Figure 11. The predicted variation of Nusselt number with height at (a) $x = 1/4$ and (b) $x = 3/4$ for different apertures for a water-filled cavity of aspect ratio 1/2 with an aluminium partial divider at a Rayleigh number of 10^9. Note that the top of the cavity is at $y = 1/2$

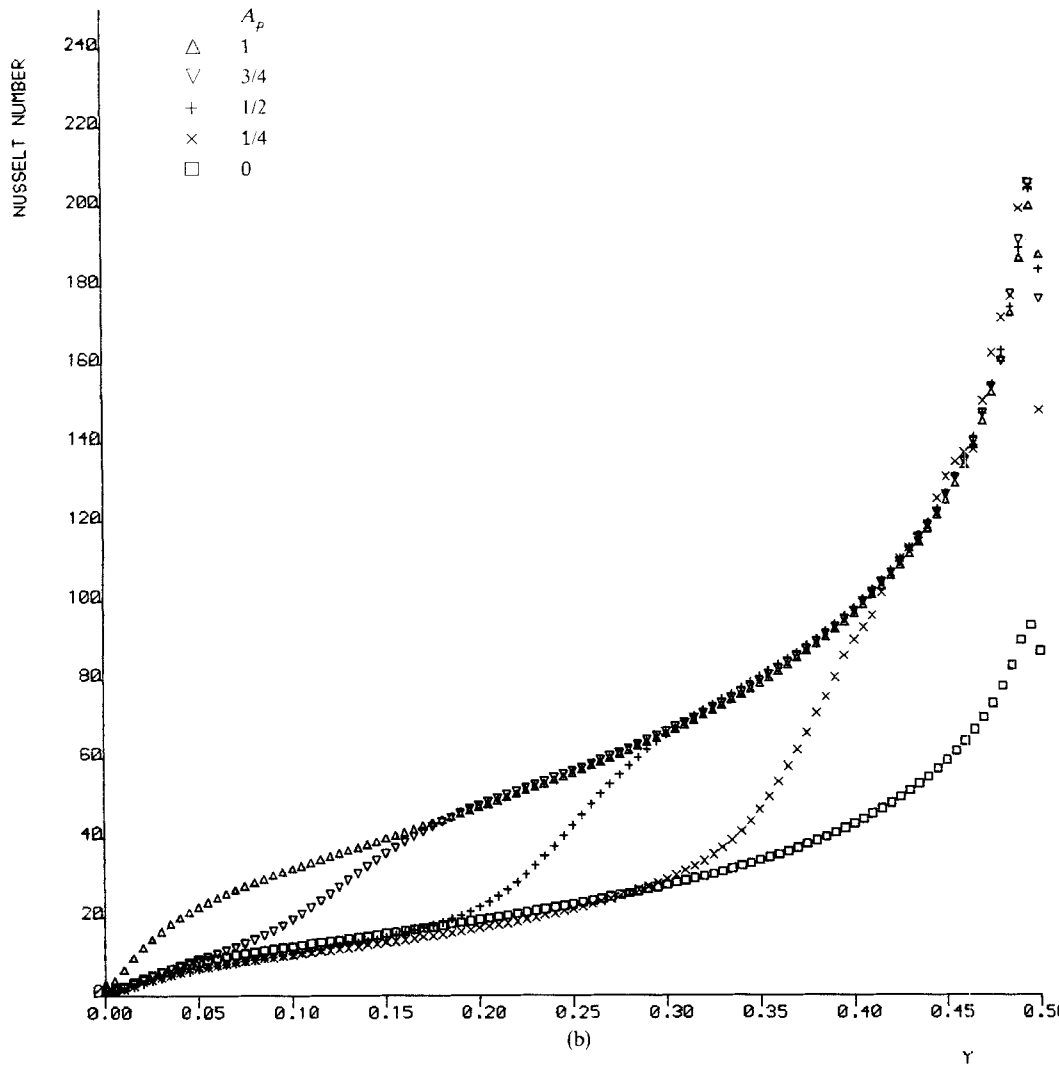
A_p
1
3/4
1/2
1/4
0
NUSSELT NUMBER
240
220
200
180
160
140
120
100
80
60
40
20
0
0.00
0.05
0.10
0.15
0.20
0.25
0.30
0.35
0.40
0.45
0.50
Y

(b)

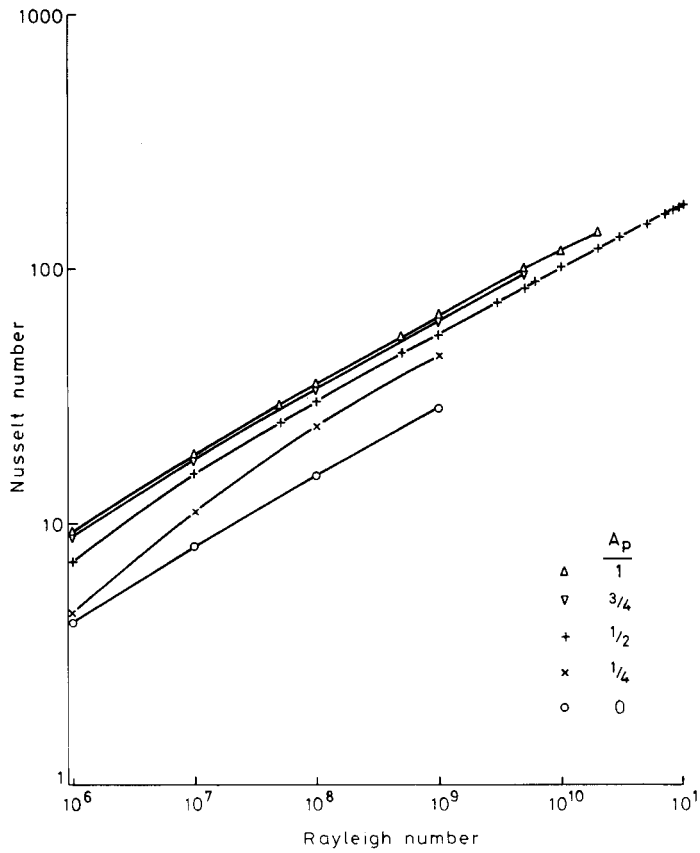

Figure 12. The variation of the average Nusselt number with Rayleigh number for a water-filled cavity of aspect ratio 1/2 with an aluminium partial divider for apertures from $A_p = 0$ to 1

undivided cavity by 15%, but the complete aluminium divider affords a reduction in heat transfer of 56% that of the undivided cavity.

At $Ra = 10^9$ the relationship between $\overline{Nu}$ and A_p is well described by

$$\overline{Nu} = 67{\cdot}1\, A_p^{0.265}$$

for the aluminium divider with $0{\cdot}25 \leqslant A_p \leqslant 1{\cdot}0$; this correlation fits the predicted values to better than 2%. Nansteel and Greif[2] found a slightly smaller increase in Nusselt number with aperture at $Ra = 10^{10}$, with $\overline{Nu}$ varying as $A_p^{0.256}$.

The predicted heat transfer in the undivided cavity can be compared with other work at similar Rayleigh numbers. Bauman *et al.*[13] report a measured Nusselt number of 79 and a computed value (on a coarse grid) of 105 at $Ra = 2.4 \times 10^9$, compared with the present value of 65.9 at $Ra = 10^9$. Gadgil *et al.*[16] find 5% agreement with Nansteel and Greif,[2] but did not report results as low as 10^9.

The present results are summarised in Table II.

The effect of partition conductivity

Nansteel and Greif[2] used two contrasting types of divider in their experiments, with conductivities relative to water which made them either conducting or insulating, and showed that

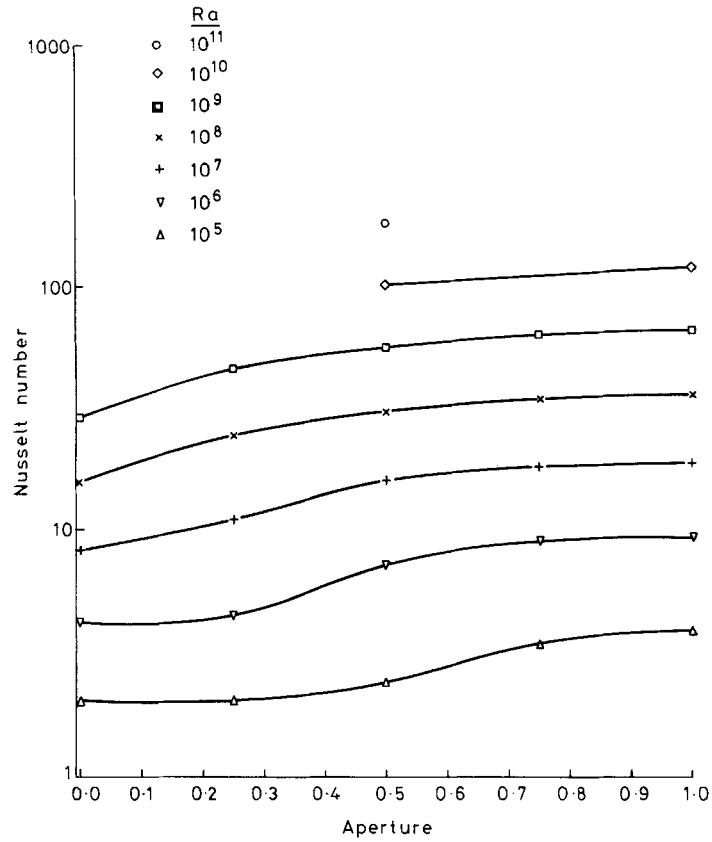

Figure 13. The variation of the average Nusselt number with aperture for a water-filled cavity of aspect ratio 1/2 with an aluminium partial divider at Rayleigh numbers from 10^5 to 10^{11}

Table II. Heat transfer in a water-filled cavity of aspect ratio 1/2 with an aluminium partial divider at $Ra = 10^9$ for different apertures

Aperture	Grid	Predicted $\overline{Nu}$
1	24 × 24	66·0
3/4	50 × 24	63·1
1/2	70 × 32	56·2
1/4	50 × 24	46·1
0	50 × 24	28·9

the conductivity of the partial divider had a significant effect on the flow and heat transfer. The insulating partition was constructed from polystyrene foam with a thin stainless steel cladding. We consider therefore the effect of reducing the relative conductivity of the partial divider in our simulation from the value of $k_r = 350$ for aluminium to $k_r = 0{\cdot}05$ corresponding to foam.

Figure 14(a) shows the predicted streamlines and isotherms for the foam 1/2-divider in water at $Ra = 10^9$. The most striking feature of the flow is the absence of any significant recirculation in the

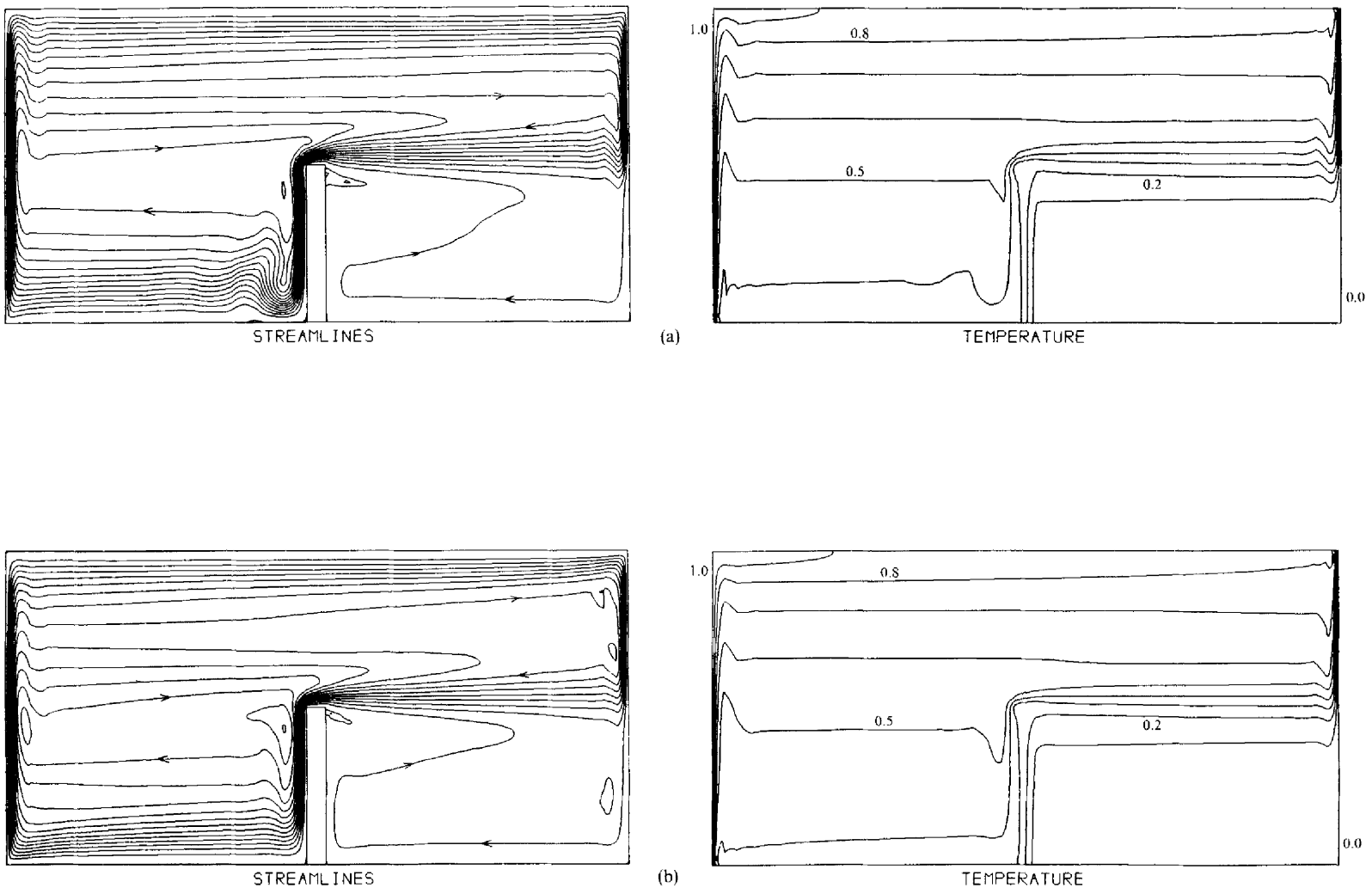

Figure 14. The predicted streamlines and isotherms in a cavity of aspect ratio 1/2 filled with (a) water and (b) silicone oil with a foam 1/2-divider at a Rayleigh number of 10^9

lower right section. Otherwise, the flow is similar to that for aluminium shown in Figure 4, with characteristic parallel flow and a jet returning from the cold wall at divider height. This is in excellent agreement with the observations of Nansteel and Greif[2] at $Ra > 10^{10}$, who noted that the foam divider suppressed almost entirely the recirculation in the region shielded from the hot wall by the divider. The isotherms show that the lower right section is considerably more uniform in temperature than for aluminium, much of it being less than 0·1. There is little effect on the temperature in the upper right of the cavity, and there is consequently a larger vertical temperature gradient at divider height than was found for the aluminium divider.

As regards the overall heat transfer, Nansteel and Greif showed that for a specific size of partition the foam gave a greater reduction of heat transfer than the aluminium. However, the dependence of Nusselt number on Rayleigh number was found to be the same for both aluminium and foam partitions. The dependence of Nusselt number on aperture is, of course, different for the two contrasting materials; $\overline{Nu}$ is independent of conductivity in the limit of the undivided cavity $A_p = 1$. On the other hand, for the completely divided cavity $A_p = 0$, $\overline{Nu}$ equals the conductive heat transfer across the partition and depends strongly on its conductivity.

In Figure 15 we show the predicted dependence of the average Nusselt number on conductivity at a Rayleigh number of 10^8 for each of the apertures 0, 1/4, 1/2, 3/4 and 1. For the 1/2-divider the effect of decreasing k_r is small; for example, replacing the aluminium by foam reduces the heat transfer by 5%. For an aperture of 1/4 there is a greater reduction of 18% in substituting the foam

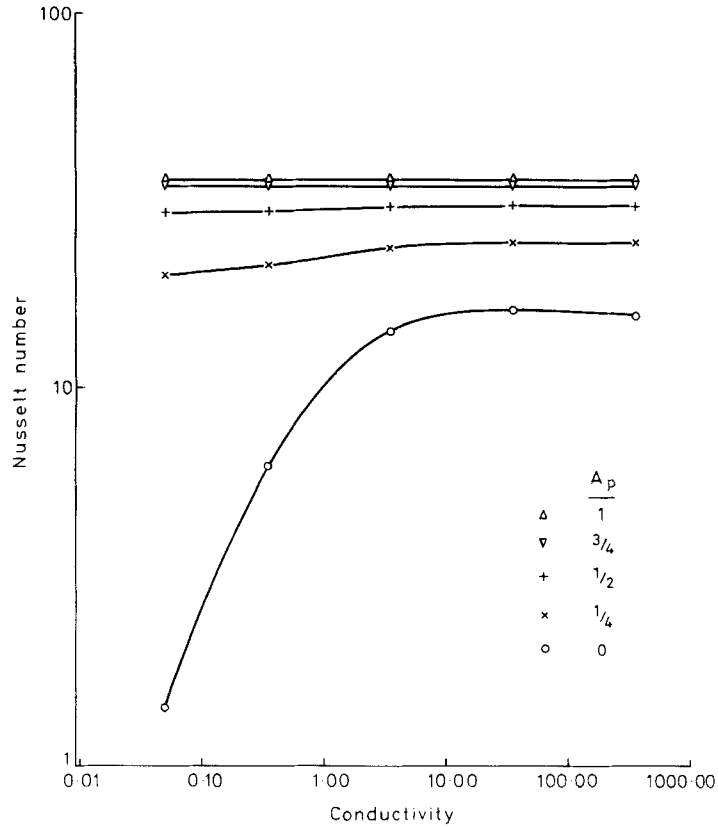

Figure 15. The variation of the average Nusselt number with relative divider conductivity for different apertures for a water-filled cavity of aspect ratio 1/2 with an aluminium partial divider at a Rayleigh number of 10^8

for the aluminium divider. The most dramatic effect is, of course, for the completely divided cavity $A_p = 0$, where there is an increasingly rapid reduction in heat transfer as k_r is decreased below 5. The correlation derived by Nansteel and Greif [2] from their measurements shows a greater effect on replacing the aluminium by the foam divider. They find a reduction of 12% for the 1/2-divider and 24% for the aperture of 1/4.

Figure 16 displays the dependence of $\overline{Nu}$ on the aperture for different conductivities. As explained, the various curves have the same limiting value at $A_p = 1$, and a limit at $A_p = 0$ which depends strongly on conductivity. The relationship between $\overline{Nu}$ and A_p is

$$\overline{Nu} = 37{\cdot}5 A_p^{0.437}$$

for the foam partition at $Ra = 10^8$. The correlation fits the predicted data to better than 5% only; we find that a power law type of relationship becomes increasingly poor as conductivity is reduced. We recall that we found

$$\overline{Nu} = 67{\cdot}1 A_p^{0.265}$$

for the aluminium partition at $Ra = 10^9$. Nansteel and Greif[2] measured a slightly larger variation of the Nusselt number with aperture and obtained exponents of 0·473 and 0·256 for the foam and aluminium dividers respectively.

The present predictions of the overall heat transfer are summarized in Table III.

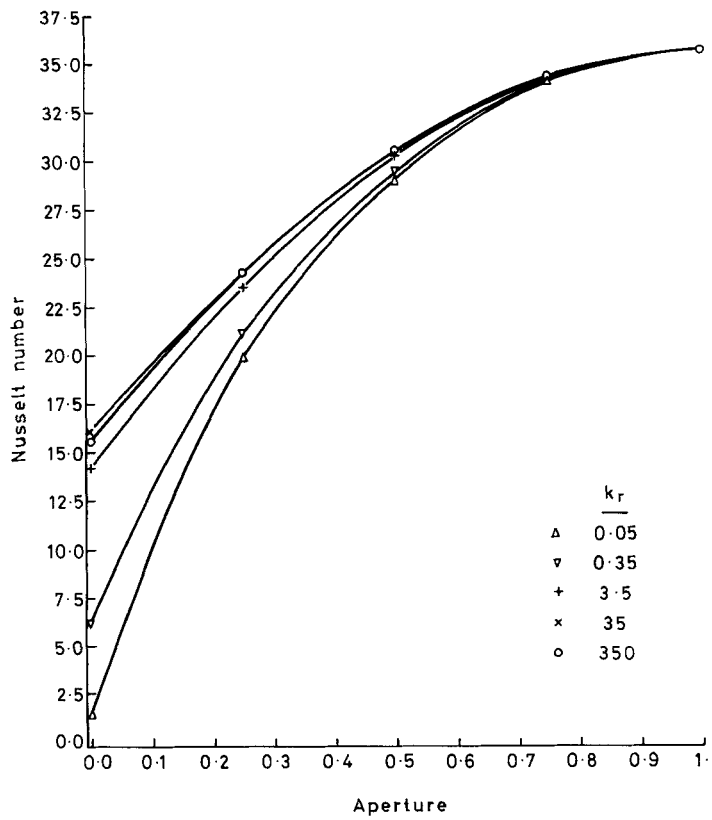

Figure 16. The variation of the average Nusselt number with aperture for a water-filled cavity of aspect ratio 1/2 with an aluminium partial divider at a Rayleigh number of 10^8 for various relative divider conductivities

Table III. Heat transfer in a water-filled cavity of aspect ratio 1/2 at $Ra = 10^8$ for different aperture and divider conductivity

Aperture	k_r	Grid	Predicted $\overline{Nu}$
0	350	34 × 16	15·6
0	35	34 × 16	16·1
0	3·5	34 × 16	14·1
0	0·35	34 × 16	6·14
0	0·05	34 × 16	1·36
1/4	350	34 × 16	24·2
1/4	35	34 × 16	24·2
1/4	3·5	34 × 16	23·5
1/4	0·35	34 × 16	21·1
1/4	0·05	34 × 16	19·8
1/2	350	34 × 16	30·5
1/2	35	34 × 16	30·4
1/2	3·5	34 × 16	30·2
1/2	0·35	34 × 16	29·4
1/2	0·05	34 × 16	29·1
3/4	350	34 × 16	34·3
3/4	35	34 × 16	34·3
3/4	3·5	34 × 16	34·3
3/4	0·35	34 × 16	34·1
3/4	0·05	34 × 16	34·1
1	—	18 × 18	35·7

Effect of fluid Prandtl number

Following their experiments with water, Nansteel[4] and Nansteel and Greif[10] studied natural convection in an oil-filled cavity of aspect ratio 1/2 with a foam partial divider and found considerable differences from the water/foam case. This is surprising since, as they point out, it is generally accepted that the Nusselt number has a very small dependence on Prandtl number in the range $1 \leqslant Pr < 10^3$. We consider therefore the effect of changing the Prandtl number in our simulation. Figure 14(b) shows the streamlines and isotherms for a foam 1/2-divider in silicone oil at a Rayleigh number 10^9. The Prandtl number was assumed to be 750, and a value of 0·24 was adopted for the conductivity of foam relative to oil. The flow shows some differences from the corresponding predictions of Figure 14(a) for a foam 1/2-divider in water, mainly in the upper right where the oil is more stagnant than the water. The isotherms do not differ in any significant way.

Clearly the comparison of a foam partial divider in oil with that in water does not reveal the effect of Prandtl number only; the conductivity of foam relative to water is different from its conductivity relative to oil, and we have already seen the potential sensitivity of the heat transfer to k_r. The effect of the Prandtl number alone may be isolated by considering an undivided cavity, for which Nansteel and Greif also carried out measurements. We have simulated the convection of silicone oil in an undivided cavity at Rayleigh numbers of 10^9, $1{\cdot}74 \times 10^9$ and 10^{10} and find a very small variation of heat transfer with Prandtl number. For example, a Nusselt number of 65·9 was predicted for water at 10^9, whereas for silicone oil we find $\overline{Nu} = 66{\cdot}3$, an increase of less than 1%. This insensitivity to Prandtl number is in accord with the results of previous work,[17,18] but does not

agree with the measurements of Nansteel and Greif.[10] In particular we predict a Nusselt number of 77·1 for the undivided cavity at the experimental Rayleigh number of $1{\cdot}74 \times 10^9$ and Prandtl number of 830, compared with the measured value of 98·1, which is 27% higher than predicted. In addition, for silicone oil Nansteel and Greif[10] find a different variation of $\overline{Nu}$ with Ra, whereas we predict the same variation with Ra for both oil and water.

Effect of aspect ratio

The predictions reported so far in this paper have been at a fixed aspect ratio of 1/2. A detailed study of the effect of the aspect ratio on the flow and heat transfer in the partially divided cavity is beyond the scope of the present study. Nevertheless, it is important to obtain some indication of the aspect ratio dependence in the light of the results of Lin and Bejan;[5] these authors measured Nusselt numbers for the partially divided water-filled cavity which are around one third lower than those of Nansteel and Greif [2] and the present work. Lin and Bejan suggest that the smaller aspect ratio of 0·305 used in their experiments could explain the discrepancy. They used a different type of partition, consisting of a double-glazed glass/air panel, and the discrepancy in measured heat transfer was found for both the partially divided and undivided cavities.

In order to isolate the effect of cavity aspect ratio from that of divider conductivity we have considered the undivided cavity $A_p = 1$ only. Figure 17 shows the flow and isotherms at the aspect ratio of 0·305 used by Lin and Bejan at one of their experimental Rayleigh numbers of $6{\cdot}13 \times 10^{10}$. The flow has strong boundary layers, with parallel streamlines away from the sidewalls, and there is stable temperature stratification throughout much of the cavity. These characteristics are in good agreement with the predictions of Tichy and Gadgil,[19] and there is no indication of the horizontal

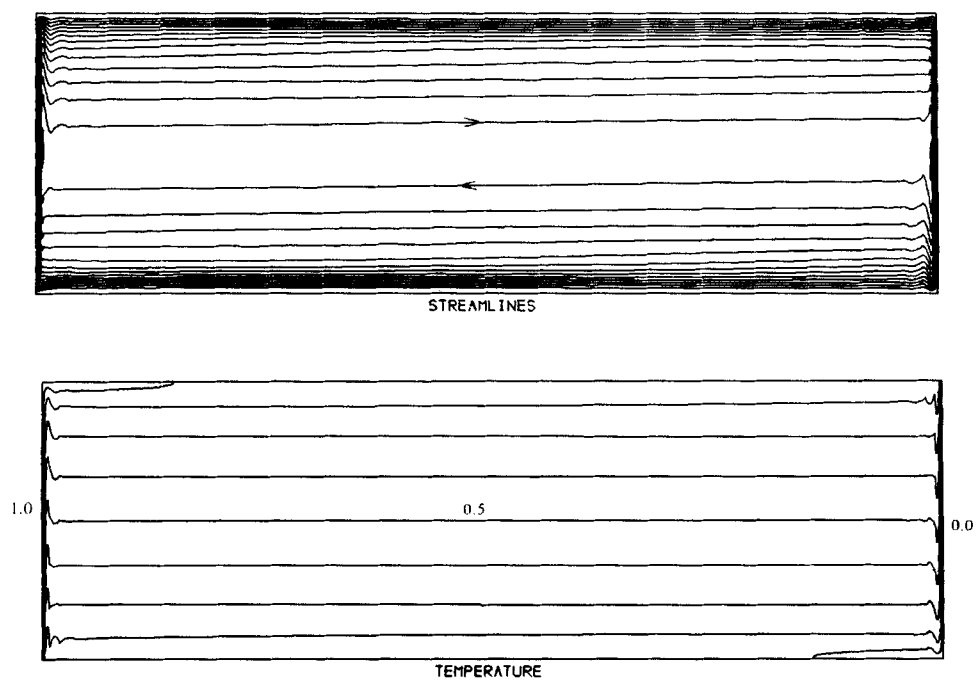

Figure 17. The predicted streamlines and isotherms in an undivided water-filled cavity of aspect ratio 0·305 at a Rayleigh number of $6{\cdot}13 \times 10^{10}$

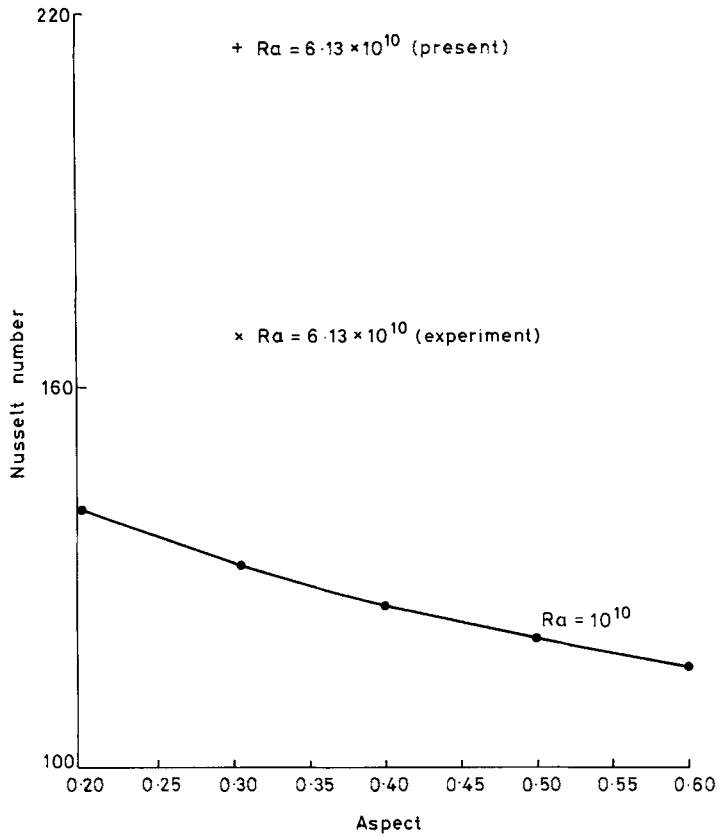

Figure 18. The variation of the average Nusselt number with aspect ratio for an undivided water-filled cavity with an aluminium partial divider: ●, predicted at $Ra = 10^{10}$; +, predicted at $Ra = 6.13 \times 10^{10}$; ×, measured (Lin and Bejan[5] at $Ra = 6.13 \times 10^{10}$

intrusions of reverse flow observed by Bejan *et al.*[20] in a different study at lower aspect ratio. The predicted Nusselt number is 214 for $A = 0{\cdot}305$ and $Ra = 6{\cdot}13 \times 10^{10}$, compared with the value of 168 measured by Lin and Bejan, which is 22% lower than predicted.

The heat transfer is shown in Figure 18 as a function of aspect ratio for $0{\cdot}2 \leqslant A \leqslant 0{\cdot}6$ at $Ra = 10^{10}$ in the undivided water-filled cavity. We find that the heat transfer *increases* with decreasing aspect ratio, so that the discrepancy between the Nusselt numbers of Lin and Bejan at $A = 0{\cdot}305$ and the larger values of Nansteel and Greif and of the present work at $A = 0{\cdot}5$ is increased when an appropriate adjustment for the different aspect ratios is made. The dependence of predicted Nusselt number on aspect ratio is moderate and is well approximated by

$$\overline{Nu} = 106 A^{-0{\cdot}181}$$

for $0{\cdot}2 \leqslant A \leqslant 0{\cdot}6$ at $Ra = 10^{10}$, which fits the predicted data to better than 1%. The Nusselt number at $A = 0{\cdot}305$ is about 15% larger than at $A = 0{\cdot}6$.

As regards the comparison with other work, the correlation of Inaba *et al.*[18] shows a very small variation of Nusselt number with aspect ratio. When converted to the scaling used here, it has the form $A^{-0{\cdot}06}$ for aspect ratios in the range $0{\cdot}2 \leqslant A \leqslant 1{\cdot}0$ at lower Rayleigh number. However, the values of the Nusselt number extrapolated to a Rayleigh number of 10^{10} are about half the present values. The measurements of Wirtz *et al.*[21] at $A = 0{\cdot}1$ and $0{\cdot}2$ also show a small increase in Nusselt

Table IV. Heat transfer in an undivided water-filled cavity at different aspect ratio and Rayleigh number

Rayleigh number	Aspect ratio	Grid	Predicted $\overline{Nu}$	Measured $\overline{Nu}$
10^{10}	0·6	24 × 24	115	—
10^{10}	0·5	24 × 24	120	—
10^{10}	0·4	24 × 24	125	—
10^{10}	0.305	24 × 24	132	—
10^{10}	0·2	24 × 24	141	—
$6{\cdot}1 \times 10^{10}$	0·305	24 × 24	214	168*
2×10^{10}	0·2	24 × 24	171	162†

* Reference 5.
† Reference 21.

number with decreasing aspect ratio. We have carried out a calculation at $A = 0{\cdot}2$ and $Ra = 2 \times 10^{10}$ at the lower end of the range of experimental Rayleigh numbers considered by Wirtz *et al.* and find a Nusselt number of 171. This agrees well with the value of 162 obtained from the correlation of Wirtz *et al.* at the same aspect ratio and Rayleigh number. We note that the calculations of Gadgil *et al.*[16] are also in agreement with the measurements of Nansteel and Greif[2] for $A = 0{\cdot}5$ and with those of Wirtz *et al.*[21] at $A = 0{\cdot}2$.

The present predictions of the overall heat transfer are summarised in Table IV.

CONCLUSIONS

Predictions of laminar natural convection inside a partially divided rectangular cavity at high Rayleigh number have been presented, and the effects of Rayleigh number, divider height, divider conductivity, fluid Prandtl number and cavity aspect ratio have been assessed.

The high Rayleigh number regime identified by Nansteel and Greif[2] has been confirmed and found to extend from around $Ra = 10^9$ to at least 10^{11}. The predicted flows in this regime show a characteristic behaviour in agreement with experiment and differing significantly from previous results at lower Rayleigh number. The flow is characterized by narrow boundary layers, weak core flow and separation of the cold wall boundary layer at divider height, with a resulting jet returning from the cold wall to the tip of the partial divider. In the high Rayleigh number region the overall heat transfer is accurately described by a simple power law relationship $\overline{Nu} = 0{\cdot}286 Ra^{0{\cdot}255}$ for an aluminium half-divider in water. There is good agreement between the predicted and measured Nusselt numbers, although Nansteel and Greif find a different dependence of $\overline{Nu}$ on Ra.

The height of the aluminium partial divider in the water-filled cavity was varied between 0 and 1, and for each aperture results were obtained for Rayleigh numbers in the range 10^5 to 10^9. At $Ra = 10^9$ the characteristic cold jet returning from the cold wall to the divider tip was found to intensify as the aperture increased. The predicted variation of the heat transfer with A_p is $\overline{Nu} = 67{\cdot}1\, A_p^{0{\cdot}265}$, which is close to that measured by Nansteel and Greif.

The effect of varying the conductance was investigated at a Rayleigh number of 10^8 for apertures in the range 0 to 1. As the aperture decreases, a smaller conductivity becomes increasingly effective at reducing the heat transfer in the cavity. For fixed aperture the predicted reduction in heat transfer afforded by replacing the aluminium with foam was smaller than measured by Nansteel and Greif.

The natural convection of silicone oil in an undivided cavity was simulated, and the heat transfer differed negligibly from the corresponding results for water. This agrees with previous analyses but disagrees with the experiments of Nansteel and Greif,[10] who found larger Nusselt numbers for oil than for water and a greater increase with Rayleigh number.

The convection of water in an undivided cavity with aspect ratios in the range 0·2 to 0·6 was studied at $Ra = 10^{10}$. A small variation of Nusselt number with aspect ratio was found, and the predicted heat transfer was higher than measured by Lin and Bejan[5] for $A = 0{\cdot}305$, but in accord with that measured by Wirtz *et al.*[21] for $A = 0{\cdot}2$. The overall heat transfer is well described by $\overline{Nu} = 106A^{-0{\cdot}181}$.

In summary, a direct simulation of the laminar natural convection in a partially divided cavity has been carried out for realistic operating conditions. This work demonstrates that such a simulation, when combined with experimental studies, can offer a powerful tool for understanding the complex phenomena that occur in highly convective flows and for deriving their heat transfer characteristics.

REFERENCES

1. D. Duxbury, 'An interferometric study of natural convection in enclosed plane air layers with complete and partial central vertical divisions', *Ph.D. Thesis*, University of Salford, U.K., 1979.
2. M. W. Nansteel and R. Greif, 'Natural convection in undivided and partially divided rectangular enclosures', *J. Heat Transfer*, **103**, 623–629 (1981).
3. M. W. Nansteel and R. Greif, 'An investigation of natural convection in enclosures with two- and three-dimensional partitions', *Int. J. Heat Mass Transfer*, **27**, 561–571 (1984).
4. M. W. Nansteel, 'Natural convection in enclosures', *Ph.D. Dissertation*, University of California, Berkeley, U.S.A., 1982.
5. N. N. Lin and A. Bejan, 'Natural convection in a partially divided enclosure', *Int. J. Heat Mass Transfer*, **26**, 1867–1878 (1983).
6. S. M. Bajorek and J. R. Lloyd, 'Experimental investigation of natural convection in partitoned enclosures', *J. Heat Transfer*, **104**, 527–532 (1982).
7. L. C. Chang, J. R. Lloyd and K. T. Yang, 'A finite difference study of natural convection in complex enclosures', *Proc. 7th Int. Heat Transfer Conf.* Munich, West Germany, 1982, Paper NC11, pp. 183–188.
8. K. H. Winters, 'The effect of conducting divisions on the natural convection of air in a rectangular cavity with heated sidewalls', *Proc. 3rd. Joint AIAA/ASME Thermophysics, Fluids, Plasma and Heat Transfer Conf.* St. Louis, Missouri, U.S.A., 1982, Paper 82-HT-69.
9. K. H. Winters, 'Laminar natural convection in a partially divided cavity', *Harwell Report AERE TP. 990*, 1983; and *Proc. 3rd. Int. Conf. on Numerical Methods in Thermal Problems* Seattle, Washington, U.S.A., 1983, pp. 563–573.
10. M. W. Nansteel and R. Greif, 'Natural convection heat transfer in complex enclosures at large Prandtl number', *J. Heat Transfer*, **105**, 912 (1983).
11. K. A. Cliffe, C. P. Jackson and K. H. Winters, 'Natural convection at very high Rayleigh numbers', *Harwell Report AERE TP. 1037*, 1985; and *J. Comput. Phys.*, **60**, 155–160 (1985).
12. M. S. Bohn, A. T. Kirkpatrick and D. A. Olson, 'Experimental study of three-dimensional natural convection at high Rayleigh number', *J. Heat Transfer*, **106**, 339–345 (1984).
13. F. Bauman, A. Gadgil, R. Kammerud and R. Greif, 'Buoyancy driven convection in rectangular enclosures: experimental results and numerical calculations', *Proc. Joint ASME/AIChE National Heat Transfer Conf.*, Orlando, Florida, U.S.A., 1980, Paper 80-HT-66.
14. G. Kenworthy, G. L. Quarini, K. H. Winters, N. Sheriff and D. A. Booth, 'Study of natural convection phenomena in an LMFBR intermediate plenum', *Proc. 3rd Int. Conf. on Liquid Metal Engineering and Technology in Energy Production, Vol. 1*, Oxford, U.K., 1984, BNES, London, pp. 167–172.
15. P. L. Betts and V. Haroutunian, 'A stream function finite element solution for two-dimensional natural convection with accurate representation of Nusselt number variations near a corner', *Int. j. numer. methods fluids*, **3**, 605–622 (1983).
16. A. Gadgil, F. Bauman, E. Altmayer and R. C. Kammerud, 'Verification of a numerical simulation technique for natural convection', *J. Solar Energy Eng.*, **106**, 366–369 (1984).
17. G. de Vahl Davis, 'Laminar natural convection in an enclosed rectangular cavity', *Int. J. Heat Mass Transfer*, **11**, 1675–1693 (1968).
18. H. Inaba, N. Seki, S. Fukusako and K. Kanayama, 'Natural convective heat transfer in a shallow rectangular cavity with different end temperatures', *Numer. Heat Transfer*, **4**, 459–468 (1981).
19. J. Tichy and A. Gadgil, 'High Rayleigh number laminar convection in low aspect ratio enclosures with adiabatic horizontal walls and differentially heated vertical walls', *J. Heat Transfer*, **104**, 103–110 (1982).

20. A. Bejan, A. A. Al-Homoud and J. Imberger, 'Experimental study of high-Rayleigh-number convection in a horizontal cavity with different end temperatures', *J. Fluid Mech.*, **109**, 283–299 (1981).
21. R. A. Wirtz, J. Righi and F. Zirilli, 'Measurements of natural convection across tilted enclosures of aspect ratio 0·1 and 0·2', *J. Heat Transfer*, **104**, 521–526 (1982).